UC San Diego
UC San Diego Electronic Theses and Dissertations

Title
Passive Acoustic Techniques Using Sources of Opportunity /

Permalink
https://escholarship.org/uc/item/4x761654

Author
Verlinden, Christopher M.A.

Publication Date
2014

Peer reviewed|Thesis/dissertation

UNIVERSITY OF CALIFORNIA, SAN DIEGO

Passive Acoustic Techniques Using Sources of Opportunity

A thesis submitted in partial satisfaction of the
requirements for the degree
Master of Science

in

Oceanography

by

Christopher M.A. Verlinden

Committee in charge:

William A. Kuperman, Chair
Bruce D. Cornuelle
William S. Hodgkiss

2014

The thesis of Christopher M.A. Verlinden is approved, and it is acceptable in quality and form for publication on microfilm and electronically:

_____

_____

_____
Chair

University of California, San Diego

2014

TABLE OF CONTENTS

LIST OF FIGURES

viii

ACKNOWLEDGEMENTS

ABSTRACT OF THE THESIS

Passive Acoustic Techniques Using Sources of Opportunity

by

Christopher M.A. Verlinden

Master of Science in Oceanography

University of California, San Diego, 2014

Professor William A. Kuperman, Chair

Recently in the field of Ocean Acoustics there has been a movement towards the use of passive, rather than active techniques for localizing acoustic sources and extracting information about the environment. Ships, which can be tracked using the Automatic Identification System (AIS) represent an underutilized acoustic Source of Opportunity that can potentially be used to localize sources, invert for environmental parameters, and extract information about the ocean environment such as the local time dependent Green's Function. This thesis demonstrates an application of using surface ships as a source of opportunity in source localization. Previous passive source localization methods break down due to our inability to model the acoustic environment with sufficient accuracy to create reliable replica

signals; this method eliminates the need to model the waveguide by using measured, rather than modeled, replica fields. The method uses AIS ship tracking data to populate a library of replica cross-correlation vectors which are then compared to the cross-correlation of received acoustic signals on two horizontally separated hydrophones in the presence of an unknown acoustic radiator. The coordinates associated with the correlation vector from the library which most closely corresponds to the measured correlation vector must be the location of the unknown acoustic radiator. The theory is described, tested using simulations, and validated with data from a field experiment.

Chapter 1

Introduction

Recently in the field of Ocean Acoustics there has been a movement towards the use of passive, rather than active, acoustic techniques for ocean sensing. This is partially driven by environmental regulations prohibiting the use of loud potentially disruptive active acoustic sources traditionally used in ocean sensing, and partially motivated by cost and energy savings associated with passive acoustic techniques. Passive techniques require only hydrophones and no energetically and monetarily expensive transducers or other acoustic sources. Locating acoustic sources in the ocean using methods other than active SONAR systems has been the subject of a great deal of research. Passive source localization methods such as Matched Field Processing (MFP) have been developed since the 1970s [4]. In the 1990s acousticians introduced the concept of "Acoustic Daylight" [5]. Acoustic Daylight refers to the idea that ambient ocean noise (acoustic waves) can be thought of as analogous to the electromagnetic waves from the sun. Similar to the manner in which our eyes and brain receive and process the electromagnetic radiation from the sun to form images and gain information about our surroundings, the ambient acoustic waves refracting and reflecting throughout the world ocean can be used to extract information about, and even image the environment. There have been remarkable advances in the field of passive acoustics since the idea of Acoustic Daylight was introduced. Matched Field Processing, Passive Fathometry, and a great variety of inversion techniques have been developed with varying degrees of success. Applications of acoustic "Sources of Opportunity" such as ships, biota,

sea ice, and breaking waves have been the subject of recent study.

This thesis focuses on previously unexplored applications of currently underutilized "Sources of Opportunity" in the field of passive underwater acoustics; specifically focusing on sound generated by shipping traffic. These applications include a method of acoustic source localization using measured replica fields that will be explored in detail in chapters three, four, and five. The application of shipping noise as a source of opportunity is demonstrated by showing that acoustic sources can be localized in the ocean environment using measured correlation replica fields. The theory is described, demonstrated using acoustic simulations and models, and validated using acoustic data from a field experiment.

Chapter 2

Sources of Opportunity

In the current climate of limiting active acoustic sensing techniques, capitalizing on a variety of acoustic sources of opportunity for passive processing techniques is more important than ever. Sources of opportunity include anything that puts sound into the water. Sources include surface generated noise such as bubbles and waves, biologically generated noise such as that produced by marine mammals and fish, and mechanically generated noise from sources such as breaking and cracking ice, seismic noise, and shipping noise from surface vessel traffic. This thesis focuses primarily on noise generated from surface ships; as with recent advances in vessel tracking technology, this represents an enormous, and relatively untapped, resource for ocean acousticians.

A popular source of sound for passive acoustic processing is breaking waves, bubbles bursting, and other physical oceanographic surface effects. When this noise is modeled as an infinite screen of tiny point sources in the surface layer, it can be used in a variety of applications [6]. Noise credited to breaking waves and bubbles has been used for passive fathometry [1]. Using a vertical array, and standard beamforming techniques that will be discussed further in later sections of this thesis, researchers beamformed in the vertical direction. The output of the beamformer directed straight up was cross-correlated with the output of the beamformer directed straight down. The theory is that the noise coming from directly downward must be the noise coming from the surface propagating straight down reflected off the bottom, so the lag time of the cross-correlation between

the upward and downward propagating signals should be the travel time of the signal from the array to the bottom and back. Using an estimated sound speed (just as with active fathometry) the depth of the ocean bottom, and even sub-bottom sediment structure can be determined. Figure 2.1 shows the results from the first iteration of this project. Shown in the Figure is the output of the method using a traditional, linear, Bartlett style beamformer, as well as the results using a Minimum Variance Distortion Reduction (MVDR) beamformer; both compared to the bottom frame which shows the results from an active bottom profiler. It is clear that the results compare favorably. This represents a significant advance in the field of passive acoustics as it is a clear demonstration of a technique using passive acoustics to accomplish something that, previously was only possible using active acoustic techniques. The aim of this thesis is to explore similar applications of passive acoustic techniques to accomplish what has always been done using active techniques, specifically focusing on underutilized sources of opportunities such as ship traffic.

Noise generated by ocean surface effects is also being used to extract coherent wavefronts to construct an estimate of the local Time Dependent Green's Function (TDGF) [6]. Noise generated by cracking sea ice can be a useful source of opportunity for a variety of applications. In the arctic it is well-known that the dominant source of ambient noise comes from physical sea ice processes. There is current research being done to invert for environmental information using noise from cracking and shifting sea ice. Various biologics have been used as sources of opportunity for acoustic research in the past. Marine mammals such as whales can have source levels as high as 180 dB and clearly discernible signals that can propagate for thousands of kilometers [7]. One recent study used noise generated by croaker fish to estimate the local TDGF on a horizontal array [2]. Time delays associated with the multi-path propagation structure between elements on a bottom mounted horizontal array of hydrophones were extracted and used to estimate the local TDGF. The TDGF can inform researchers about the nature of the acoustic environment. Specifically in this study, the TDGF was used to estimate the critical angle of the ocean-bottom interface which is indicative of sediment type.
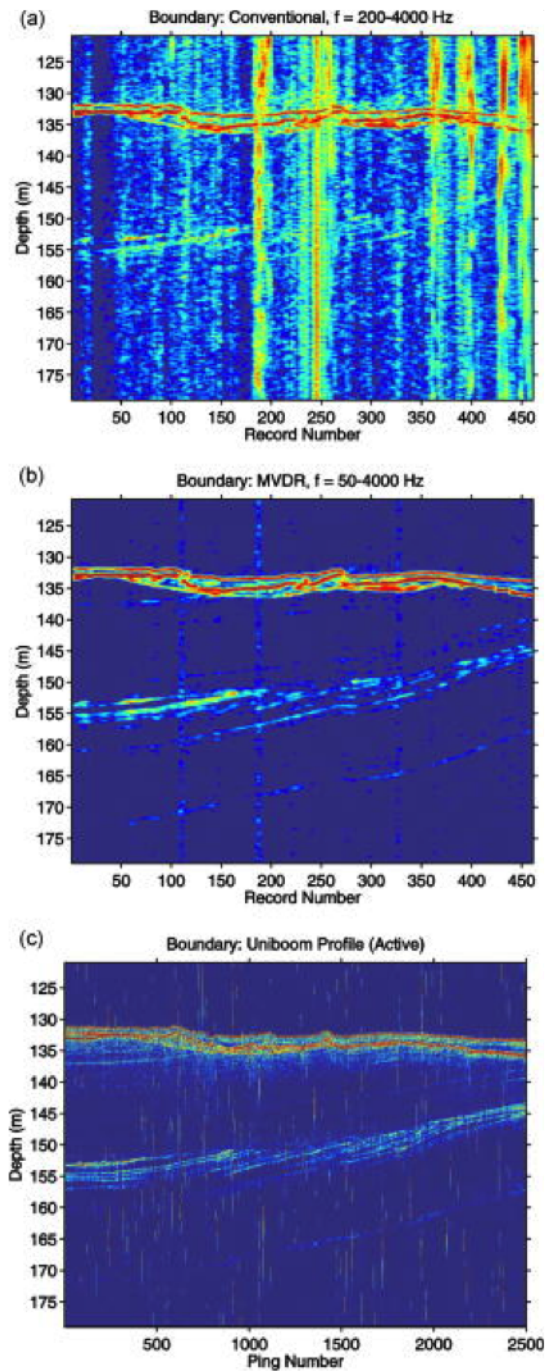
Figure 2.1: Passive Fathometer results from Siderius et al [1]. Bartlett style beamformer, as well as the results using a Minimum Variance Distortion Reduction (MVDR) beamformer are shown in the top two frames; both compare favorably with the bottom frame, which shows the results from an active bottom profiler.
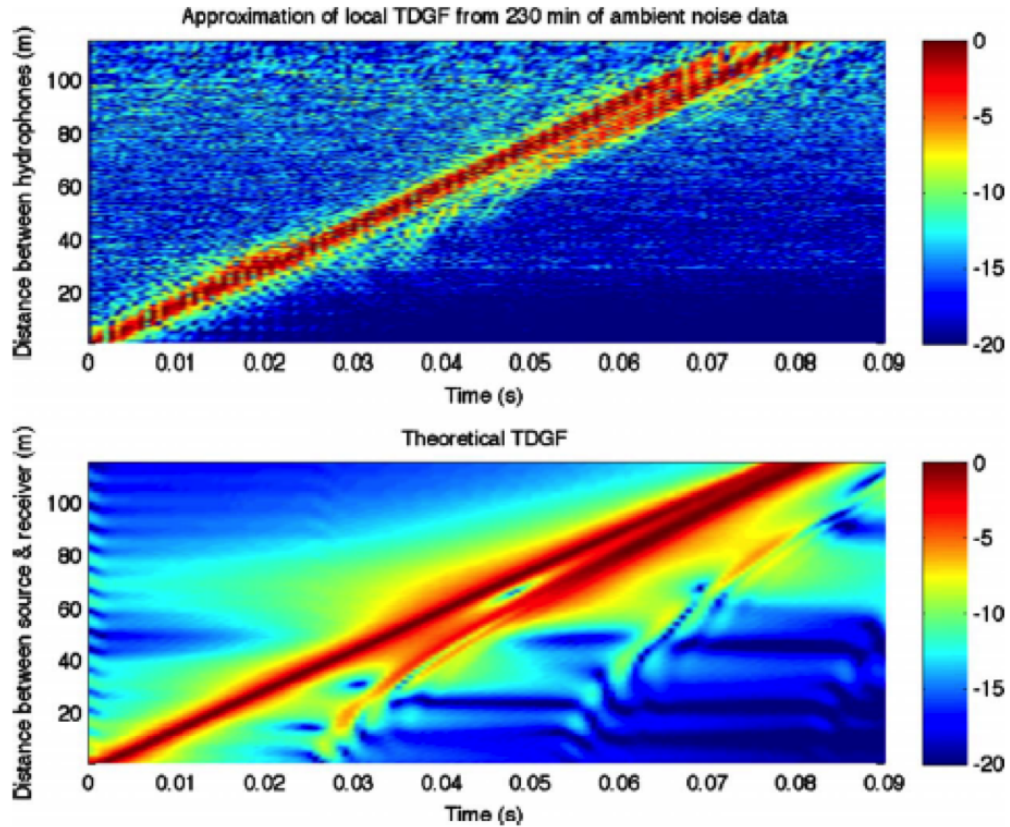
Figure 2.2: Time Dependent Green's function estimated and predicted from [2]

Figure 2.2 shows the TDGF estimated using the technique described above as well as the theoretical TDGF for the acoustic environment of the study area.

One of the primary limitations of this study was that it was difficult to build up enough coherence in the noise across the array because it was difficult to predict when the noise generated by croaker fish would be most coherent. This is where the source of opportunity that is the primary focus of this thesis comes in: shipping noise can be highly coherent across a horizontal array, especially when the ships generating the noise are crossing the end fire orientation of the array, and Ships are very easy to track. One possible application of using ships as sources of opportunity is to attempt to emulate the results of this study using shipping traffic as the source of noise instead of croaker fish; given that our knowledge of ship locations should eliminate the need to estimate the optimum time window to

use for the correlation function, as the optimum time window will be obvious (and short) due to the source ship's proximity and orientation to the array.

The dominant source of ambient ocean noise in the frequency range between 10 and 300 Hz is anthropogenic ship noise input [3]. This is clearly illustrated in the Wenz curves included in Figure 2.3. Sound in this frequency range can be extremely useful for a variety of applications, and the passive techniques used to analyze the acoustic fields generated by these ships are made more powerful with increased knowledge about the source of the radiator. Thanks to advances in ship tracking technology it is now possible to precisely track nearly all surface ships at all times. It is also possible to determine amplifying information about each ship including course, speed, and dimensions. With this information becoming available over the past decade, there is an enormous opportunity for ocean acousticians to capitalize on this data source and to apply it to a variety of acoustic techniques.

Almost all modern commercial vessels are equipped with Automatic Identification Systems (AIS). AIS is an automated system for the tracking and identification of ships designed for the purposes of collision avoidance and safety of life at sea. While it was never intended for use as a global monitoring system or for use in research applications, the data can be logged and it can be used to track ships as acoustic radiators. AIS utilizes standard Very High Frequency (VHF) radio communications to transmit name, identification number, course, speed, position, and other various data for ships equipped with the system. It is used by ships, base stations, Vessel Traffic Systems (VTS), and can be picked up by satellites. Figure 2.4 shows an overview of the AIS system. It is evident from this Figure how every station and ship acts like a repeater for every other AIS unit in the system, significantly extended its range.

AIS was originally developed in the early 1990s as a short-range identification and tracking system for avoiding vessel collisions. In 2002 the International Maritime Organization (IMO) Safety of Life at Sea (SOLAS) mandated most vessels over 300 gross tons be equipped with AIS. Over the next three years individual nations and the IMO started to implement stricter and more comprehensive mandates requiring more vessels be equipped with AIS. In 2005, some government
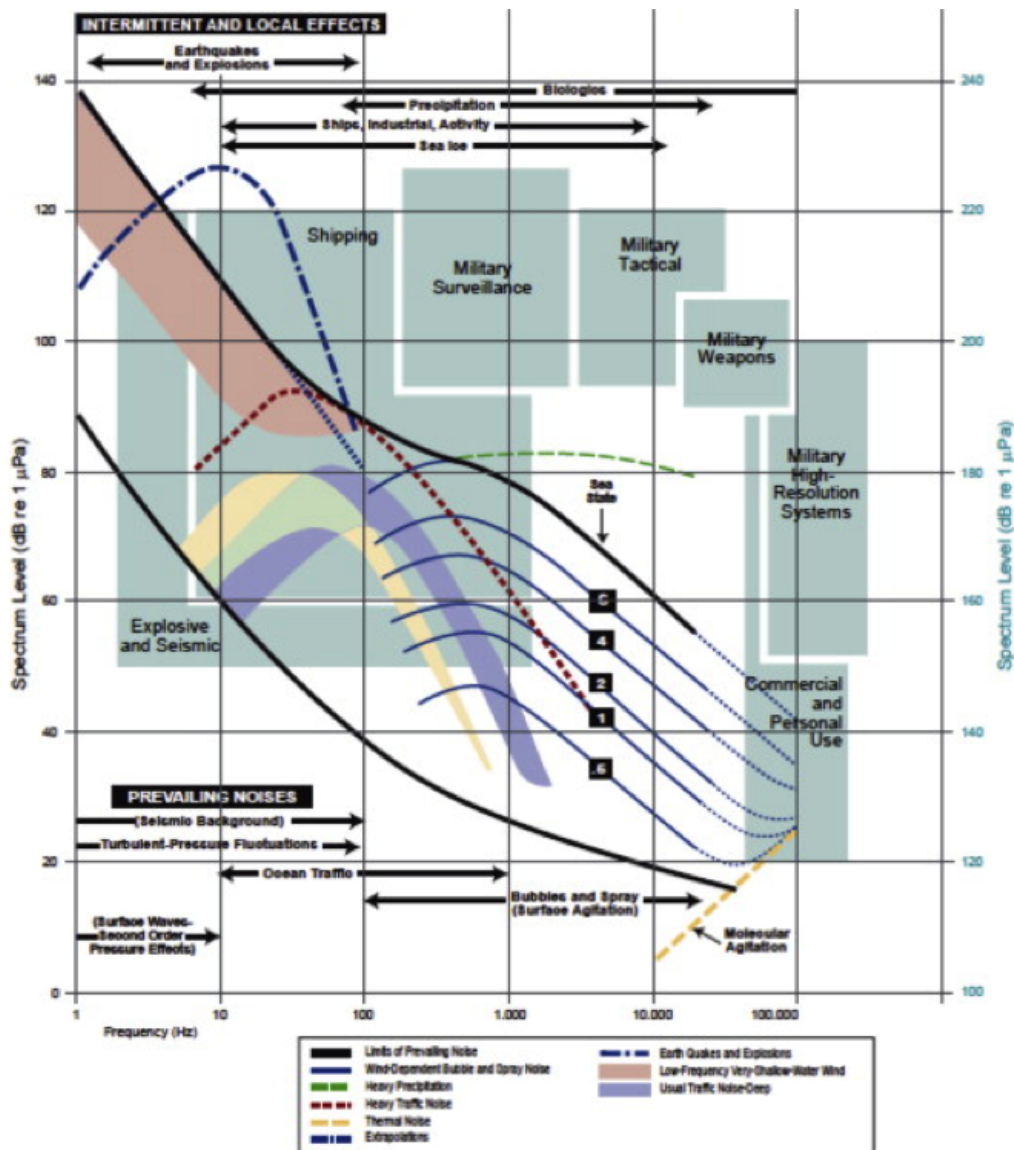
Figure 2.3: Wenz Curves showing dominant sources of ambient acoustic noise in the ocean in various frequency ranges [3].

entities and private companies began experimenting with collecting AIS data via satellite, and by 2006 most maritime nations had mandated large commercial vessels on international voyages be equipped with some form of AIS. The United states implemented regulations requiring nearly all commercial vessels operating in major ports, all vessels on international voyages, and vessels over a certain size carry AIS. In 2008 satellite AIS data started to become available for purchase over

Figure 2.4: Cartoon depicting how AIS works. Each ship acts like a repeater for every other ship, significantly extending the range of the system. Also the transmissions from individual ships can be detected by satellites.

the internet for sale by private companies operating micro-satellite constellations. By 2010, all commercial vessels in European Internal Waterways were mandated to use AIS. In 2012, over 250,000 vessels worldwide were equipped with AIS, with over one million vessels expected to be outfitted in the next few years. In 2013 and 2014 the United States and European (respectively) expanded AIS carriage requirements further and all of the aforementioned requirements became enforceable by law without exception.

Currently the IMO requires all vessels over 300 gross tons on international voyages, all vessels over 500 gross tons on domestic voyages, and all passenger vessels regardless of size be outfitted with AIS. In the United States, commercial vessels over 65 ft in length, except small passenger vessels and fishing vessels, all tanker vessels, and passenger vessels over 150 GT wishing to travel internationally

must transmit AIS. Additionally, most vessels 65 ft in length or more operating in or near a Vessel Traffic System (VTS; present in most major ports), and all towing vessels over 26 ft and more than 600 HP must always transmit AIS. Vessels classified as warships are exempt from this requirement but nearly always transmit when near areas of high vessel traffic for safety purposes. There are additional rules going into effect in the next two years in the United States and Europe that will require fishing vessels over 15 m in length, and vessels on domestic voyages to carry AIS as well.

All vessels that carry AIS must always be transmitting. This means that any vessel that could potentially operate in a Vessel Traffic System (VTS), travel internationally, or ever carry passengers must always be transmitting their location via AIS. Nearly all commercial vessels, and pleasure craft of any considerable size are transmitting on AIS, which means the location of nearly all acoustic radiators in the frequency range between about 10 and 300 Hz is known at all times. The potential applications of this knowledge are limitless.

AIS uses standard VHF Radio Communications, which means it is limited in range to nearly line of sight communications. For the 12 W class A AIS transmitters that most large vessels are equipped with, this limits the range, under ideal atmospheric conditions, to about 74 km. Under more typical conditions this number is more realistically closer to half of that. This of course depends on the height and quality of the transmitters and receivers. AIS transmissions are time multiplexed using Self-Organized Time Division Multiple Access (SOTDMA) and there are 4500 time slots per minute, which can overloaded by 400-500% by sharing time slots between ships. This system of sharing bandwidth amounts to each ship in a crowded port being able transmit their location every 2-4 seconds depending on amount of vessels in the area sharing the time slots. Larger commercial vessels equipped with Class A transmitters transmit their location every few seconds, while smaller vessels equipped with class B transmitters only transmit their location every 30 seconds. Faster moving vessels will automatically transmit their location more often (every 2 seconds) while ships at anchor only transmit every 60 seconds.

Standard AIS integrates the ships' GPS navigation system, electronic charting systems, and VHF radio transceiver. There are 27 possible types of AIS messages. For class A systems, navigational data including vessel name, Maritime Mobile Service Identity (MMSI) number, course, speed, rate of turn, position, and a time stamp in UTC seconds are transmitted every couple of seconds. The latitude and longitude can be transmitted with up to 0.0001 min precision; but is limited by the accuracy of the GPS which is accurate within 10 cm when within 370 km of land where the signal can be corrected by a Digital GPS (DGPS) tower, and accurate to within 2-15m when further offshore. In addition to navigational data transmitted every few seconds, ships equipped with class A AIS units also transmit static reports every 6 minutes, which include type of cargo, type of vessel, dimensions of the ship (to the nearest meter), surveyed location of ship's positioning system antennae (GPS) in meters from bow, stern, and port and starboard sides. Additional information transmitted in the static reports includes the type of positioning system the ship is equipped with, the draft of the ship, destination, ETA, and an optional high precision UTC time stamp. All of this information makes it possible to characterize the ship as an acoustic radiator with great precision. For example, if one was to focus on noise generated by cavitating ship's propellers for a study, it would be simple to localize the propeller to within a few meters of accuracy from the information transmitted via AIS.

AIS data is available anywhere in the world. Between government agencies that log the data from arrays of shore based radio towers, and private companies that record massive databases of satellite derived AIS ship tracking data, one could reasonably obtain AIS data for any experiment conducted from 2009 through the present. In United States' coastal waters, the United Stated Coast Guard Navigation Center (NAVCEN) Nationwide AIS (NAIS) database uses a network of 200 VHF radio transceiver towers nationwide to record all AIS data within about 100 km of the US coast for the primary purpose of Maritime Domain Awareness. In reality, data is actually available for 500-700 km offshore via the NAIS database because of the way that AIS works for ships at sea. Each ship acts as a repeater for every other ship. In other words, with a tower on shore, one could detect every

ship within 30 km, and every ship within 30 km of those ships until there is a gap in shipping coverage. Under typical coastal shipping traffic conditions, for most of the western seaboard, there is continuous coverage out to nearly 700 km. NAIS provides historical data upon request to most organizations, and institutions affiliated with the United States Government can request live-feed access to their database for real time coverage. NATO has a similar system which records AIS data along the European coast that is also sometimes available upon request.

Other sources of AIS ship tracking data include NATO's Centre for Maritime Research and Experimentation (CMRE), which records AIS ship tracking for several European and international regions for research purposes and is often willing to share their data with outside researchers. Commercial sources of AIS data include the Marine Exchange, a company that manages some Vessel Traffic Systems in the United States, ORBCOMM, ExactEarth, and Spacequest: three companies that have been recording and distributing satellite AIS ship tracking data since 2008. With few exceptions, these companies can provide AIS data anywhere in the world in a variety of formats, and they make specialized products and analysis available to paying customers. There are also open source AIS data providers that have limited coverage and availability including MarineTraffic.com, which even has a cell phone application for tracking ships.

AIS Data is originally transmitted in the standard National Marine Electronics Association (NMEA) format. There are a total of 27 different types of NMEA messages utilized by AIS systems, but we are primarily concerned with message types 1-3 which relay navigational data, and message type 5 which relays static reports including information about the ship. Figure 2.5 depicts a typical sample of NMEA data from an AIS transmission.

NMEA is computational expensive to store and process as the file sizes can easily exceed terabytes for a few hundred square km of data over a period of a couple of weeks. Additionally, NMEA is difficult to process using traditional Matlab or FORTRAN programing scripts so it is beneficial to convert the NMEA files to another format for storage and analysis. There are commercially available programs that read files directly in NMEA format and make a variety of analysis

\s:b003669978,c:1266537497*6A\\xs:rOSCDPSS,xc:1266537479*0D\!AIVDM,1,1,,B,35NB>wPPA9I=5gp@wcgrr`f000lh,0*49

\g:1-2-419843,s:r01NFIS1,c:1266537496*14\\xs:rOSCDPSS,xc:1266537479*0D\!AIVDM,1,1,,B,15N31ogP00Je;q:GB?j00?wl0@Rd,0*58

\g:2-2-419843*5E\$ARVSI,r01NFIS1,,235859.17097582,2218,-113,0*01

\g:1-2-282788,s:r05CCPH1,c:1266537482*13\\xs:rOSCDPSS,xc:1266537479*0D\!AIVDM,1,1,,A,15N4r40v@tJVRDRFhWp`Knf026s`,0*39

\g:2-2-282788*52\$ARVSI,r05CCPH1,,235859.36313653,2226,-104,0*07
\g:1-3-
237831,s:r11NPSU1,c:1266537482*14\\xs:rOSCDPSS,xc:1266537479*0D\!AIVDM,2,1,5,B,55OVcp02:PQiL=SSSS@50j10PThU10TpE>2222
16HIA,0*36

\g:2-3-237831*50\!AIVDM,2,2,5,B,DD4ao0OShBk0CQ88888888888880,2*6F

\g:3-3-237831*51\$ARVSI,r11NPSU1,5,235858.64316145,2199,-103,0*34
\g:1-2-
54765,s:b003669987,c:1266537496*2C\\xs:rOSCDPSS,xc:1266537479*0D\!AIVDM,2,1,8,B,5mNGRGP00001L@GKWO1<4pALT<f2222222
222201p71340007P00000,0*03

Figure 2.5: Sample of NMEA data from AIS transmission (from NAIS live feed).

and display tools available, but none of these programs were used in this study. For the purposes of this study I used a variety of methods to process the AIS data. First, I converted the data to Comma Separated Value format (.csv) using a homemade Python script. I simultaneously generated Keyhole Markup Language (.kml) files also using a homemade Python Script. It is important to note that when requesting historical data from NAIS, or purchasing AIS data from most commercial sources, the data can be requested already converted to .csv or .kml format. It is only when using a live feed to the NAIS database, or when pulling AIS data from the original unit or a ship's navigational computer that one needs to convert the original NMEA files. Once the data have been converted to .kml and .csv files there are a variety of options for analysis. I used ESRI's ArcGIS software to display the ship tracking data for presentation material. The .kml files were converted to ESRI shapefiles using the built in Data Conversion toolbox. ArcGIS was used to display the ship tracks in a user-friendly manner which made choosing experiment times and locations straight forward. Figure 2.6 shows a sample of AIS data converted from NMEA to .kml, then displayed using ArcGIS. The grids I chose to use for the source localization experiment, and sensor positions can easily be compared to the ship tracks when the data is displayed in this format.

MATLAB was also used to analyze the AIS ship tracking data. MATLAB is capable of uploading .csv files directly, but often these files became too cumbersome to work with, so in most cases, for the purposes of this study, the AIS ship tracking data was down-sampled by some factor, parsed into aggregate .kml files, then
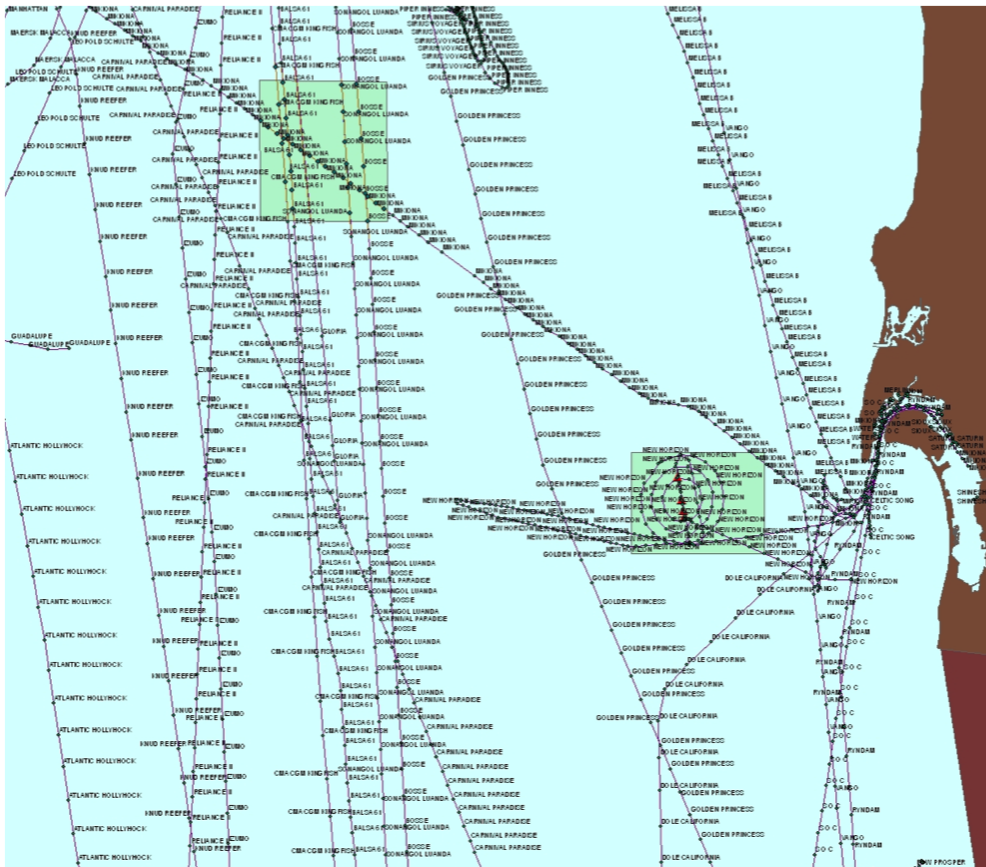
Figure 2.6: AIS Data Sample Displayed in ArcGIS.

uploaded into MATLAB as a structure for analysis using a heavily modified open source function called 'kml2struct'. This resulted in files containing ship name, position, and time, which made plotting and analysis straight forward. A 6 hour section of ship tracking data that was imported into MATLAB using the modified 'kml2struct' function is shown in Figure 2.7.

It is easy to see how the availability of tracking information for nearly all acoustic radiators in a given frequency band can be useful in the field of ocean acoustics. One simple application of this data is designing adaptive filters to remove unwanted shipping noise from acoustic experiments where this signal represents an unwanted nuisance parameter. There are a variety of potential applications of using ships as sources of opportunity in the broad field of oceanographic geo-acoustic inversions. One potential geo-acoustic inversion application of ship tracking data
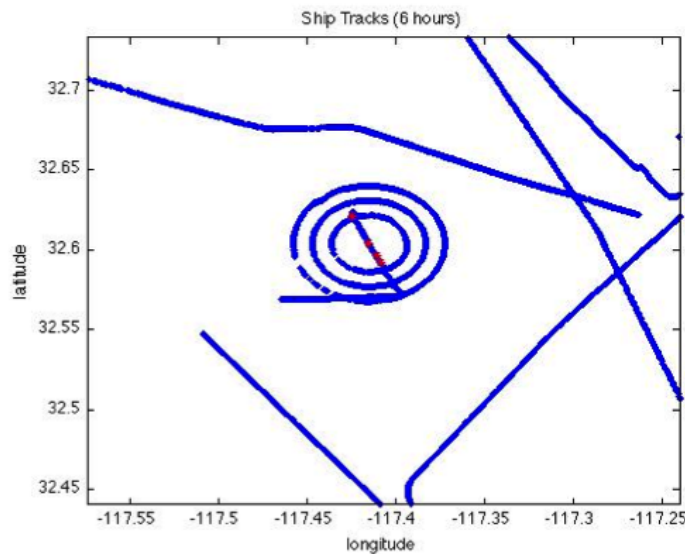
Figure 2.7: AIS Data Sample in Matlab. Ship tracks are plotted in blue over the locations of the sensors for the Noise 09 acoustic experiment (plotted in red).

is the idea of inverting for the sound speed profile of the water column, and by extension temperature and salinity parameters. This could be accomplished by parameterizing the sound speed profile in terms of empirical orthogonal functions (EOFs), and conducting standard matched field processing techniques (MFP) to localize a source (ship) of known location, then adjusting the coefficients of each EOF of the sound speed profile used in the modeled replica fields in the matched field processor until the source is localized in the correct location. The sound speed profile that results from the output EOF coefficients must then be the sound speed profile of the water column [8]. Similar methods could be applied to inverting for ocean sediment structure and composition. AIS Sip tracking data could also potentially be applied in methods designed to extract the local time dependent Green's function (TDGF) for an acoustic environment [2]. This could be done in a similar manner as in Fried et al. (2008), only using the more predictably coherent noise from shipping traffic, instead of the unpredictable noise generated by croaker fish, as was used in that study. The focus of this study is the application of AIS ship tracking data in passive source localization techniques. In the next chapter a technique for localizing acoustic sources using measured correlation vector replica

fields, associated with geographic grid points based on historical AIS ship tracking data, is explored in depth.

Chapter 3

Correlation Based Source Localization Using Measured Replica Fields – Theory

3.1 Previous Source Localization Techniques: Beamforming and Matched Field Processing

In this thesis I will demonstrate that it is possible to localize acoustic sources using the cross-correlation of signals received on separate vertical arrays correlated with a library of measured correlation replica fields. Ships transmit their location every few seconds using Automatic Identification Systems. Using the positions of these ships and correlating the signals across hydrophones separated by some arbitrary horizontal distance it is possible to assign a correlation vector taken when a ship was in a certain location to that location in a grid. By correlating signals received on the same two hydrophones at some future time with the correlation vectors (measured replica fields) saved in the library, it is possible to localize acoustic sources. This is done by determining which grid points in the library the correlation vector most closely matches; analogous to matched field processing but using measured replica fields instead of modeled replicas, and correlation vectors instead of the acoustic signal itself for comparison.

There has been a great deal of attention in recent years to localizing acoustic sources using passive, rather than active processing techniques. The most basic technique for determining the location about an acoustic radiator is standard plane wave beamforming. Beamforming is essentially listening in a certain direction. The most basic type of beamforming is linear or Bartlett beamforming. A Bartlett beamformer works by recording the acoustic signal on an array of hyrophones, creating a Cross Spectral Density Matrix (CSDM) by multiplying the the frequency domain signal on the array (one scalar value per frequency) by the complex transpose of itself, giving you an n x n CSDM. This cross spectral density matrix is then compared to a series of replica acoustic signals on the array generated using a model. The simplest manifestation of this concept is the plane wave beamformer, in which case the replicas are simply plane waves incident on the array at each possible angle. In the frequency domain this is equivalent to adding a complex exponential phase term and a cosine function for the angle of incidence. In the time domain this can be accomplished by summing the time domain signal on each element with a time delay appropriate for the path the incident wave would have to travel to move from one sensor to the next, given the incident angle. The CSDM is compared to each replica by multiplying the complex transpose of the replica vector by the CSDM then by the replica vector itself. This results in a scalar value for each replica vector; in the case of the plane wave Bartlett beamformer a scalar value for each look direction. The direction with the highest beamformer output value is the direction the source signal is coming from. The Bartlett Beamformer is described in equations 3.1 and 3.2 where d represents the data across the array; w represents the replica vector, generated using a model; K represents the CSDM; and B is the beamformer output.

$$K = d \times d^t \tag{3.1}$$

$$B = w^t K w \tag{3.2}$$

Figure 3.1 shows a typical plane wave Bartlett beamformer output (blue line). While is there a great deal of power contained within the primary lobe,

the resolution is fairly poor and there are significant side lobes. In a real-world environment with a low SNR, this method sometimes cannot resolve the direction of an acoustic radiator with sufficient accuracy.

There are many other more advanced beamforming techniques designed to increase resolution and improve SNR. One technique used in ocean acoustics is the Minimum Variance Distortion Reduction (MVDR) beamformer. The MVDR beamformer is designed to reduce the side lobes, while improving resolution. The red line in Figure 3.1 is the results of a plane wave MVDR beamformer. The minimum variance beamformer essentially makes use of the inverse of the hermitian conjugate of the cross spectral density matrix in order to amplify the central peak in precisely the direction of the incoming signal while suppressing side lobes in every other direction. Equations 3.3 and 3.4 show how the MVDR beamformer output is computed. The red line in Figure 3.1 shows the results of an MVDR beamformer for a source at 45 degrees.

$$w_{mv} = \frac{K^{-1}w}{w^t K^{-1}w} \tag{3.3}$$

$$B_{mv} = \frac{w^t K^{-1}w}{(w^t K^{-1}w)^2} = \frac{1}{w^t K^{-1}w} \tag{3.4}$$

The final equation for the MVDR beamformer output contains the inverse of the CSDM in the denominator. It is clear that if the inverse is singular then the beamformer will break down. When using simulated data for the MVDR it is necessary to add white noise to the data vectors first, which can be accomplished by adding random numbers along the diagonal of the CSDM, in order for the inverse of the matrix to not be singular and prevent the method from breaking down. If there is a slight mismatch between the data and the replica, the MVDR processor has the potential to miss the source, and the method will break down. There is another beamforming technique used in ocean acoustics designed to prevent this called the White Noise Constraint (WNC).

The WNC beamformer works where the MVDR beamformer fails because it regularizes the matrix by adding of just the right amount of white noise to the system to prevent the inverse of the CSDM from becoming singular. This is

accomplished by selecting a certain desirable white noise gain level, then solving for the appropriate adaptive (i.e. different for every look direction) quantity to add along the diagonal of the CSDM to prevent it from becoming singular. Equations 3.5, 3.6, and 3.7 show how this works. The beamformer output is calculated using a replica vector determined by adding a level of white noise to the diagonal of the CSDM as shown in 3.5 in order to satisfy the relationship in equation 3.6 with the desired white noise gain. The output of the beamformer is shown as a black line in Figure 3.1.

$$w_{wn} = \frac{(K + I\epsilon)^{-1}w}{w^t(K + I\epsilon)^{-1}w} \tag{3.5}$$

$$w_{wn}^t w = \delta^{-2} \tag{3.6}$$

$$B_{wn} = w_{wn}^t K w_{wn} \tag{3.7}$$

From equations 3.5, 3.6, and 3.7 it is apparent that with the epsilon term added along the diagonal the inverse of the CSDM will never become singular and the method will not break down due to slight mismatches between replicas and signals. This results in a wider central lobe of the beamformer output, like the Bartlett beamformer, but comparable side lobe reduction to the MVDR. It is also clear from the above equations that when an insufficient amount of noise is added to the CSDM of the WNC beamformer, the beamformer is virtually indistinguishable from the MVDR; and when too much noise is added, the beamformer essentially becomes a Bartlett beamformer. It is important to select an appropriate level of white noise gain to use in the WNC beamformer for a given dataset. The result of a plane wave WNC beamformer is shown as a black line in Figure 3.1.

All of the aforementioned beamforming techniques can be applied to more complicated scenarios than a simple plane wave in an infinite medium, as discussed above. These same techniques can be applied to real-world ocean waveguides, and used to attempt to localize acoustic sources in the marine environment. One such technique is Matched Field Processing (MFP). Matched Field Processing is a
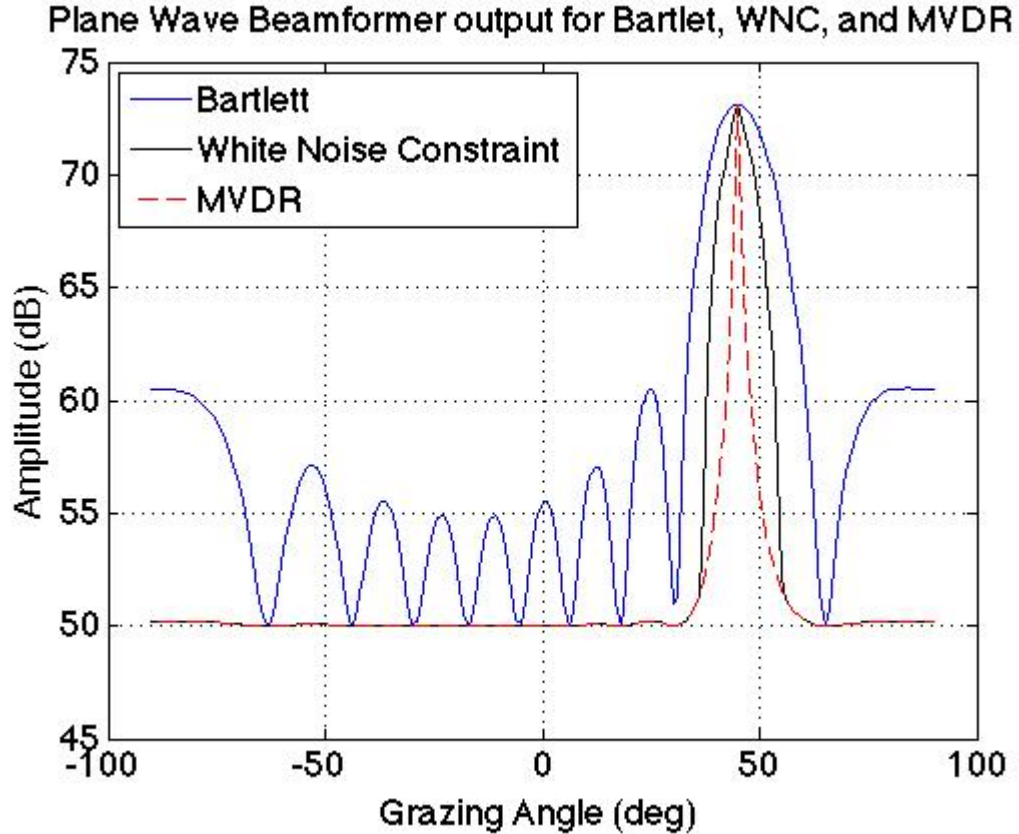
Figure 3.1: Bartlett, MVDR, and WNC Beamformers for a source at 45 degrees.

technique that involves using an acoustic propagation model such as a wavenumber integration (spectral) technique, normal mode propagation model, or parabolic equation model for estimating the expected acoustic signal on an array of elements for a waveguide of given characteristics for a source in a given location. This process is repeated for every possible source position in a grid. The replica acoustic fields on each element are compared to the actual data received on the array using either standard linear (Bartlett) beamforming, Minimum Variance Distortion Reduction (MVDR) beamforming, or White Noise Constraint (WNC) beamforming. It is essentially the same as the plane wave beamformers described above, only the model used to generate the replica fields on the array is far more complicated than a simple complex exponential and a cosine function representing different angles of arrival. Instead of having a replica for each angle of incidence, we have a replica for every possible source position in the waveguide. The replicas are generated using

a propagation model designed to represent what an acoustic signal generated in one place will look like on the array elements. There are a variety of types of propagation models to use for the creation of your replica vectors; the most common types are: wavenumber integration (spectral) techniques, normal mode propagation models, or parabolic equation models. Ray-tracing models can be adapted to generate transmission loss results, and as a result also approximate a field on an array, but as ray-trace models are considered a high frequency approximation, they are not generally used in MFP.

Spectral, or Wavenumber Integration techniques approximate the acoustic field for a source in a given location by solving for the field in discrete, horizontally stratified layers through integral transform techniques. The Normal Mode model described below approximates these integrals as the sum of discrete modes, which reduces computation time significantly while the wavenumber integration technique solves the integrals directly by quadrature [9]. In seismology these wavenumber integration techniques are sometimes called reflectivity or discrete wavenumber methods, and in underwater acoustics, when Fast Fourier Transforms (FFTs) are used to solve the spectral integrals, spectral methods are sometimes called Fast Field Programs (FFPs). The depth dependance of the field is solved using a propagator matrix. The acoustic pressure field for a given depth and range is given by equation 3.8, where p represents the acoustic pressure field for a given range r and depth z. The wavenumber is represented by k and J is the Jacobean.

$$p(r, z) = \int \frac{e^{ik_z|z|}}{ik_z} k_r J_0(k_r r) dk_r \qquad (3.8)$$

Spectral Methods are highly effective for near field calculations of the pressure field for an acoustic source because they actually solve the spectral integrals instead of approximating the integrals using residues as other methods do. Unfortunately Wavenumber Integration techniques are computationally expensive and are not practical to use for matched field processing techniques as there are a great number of replicas that need to be created, and the computational time would be prohibitive. Figure 3.2 shows a transmission loss plot for a given waveguide computed using a spectral model.
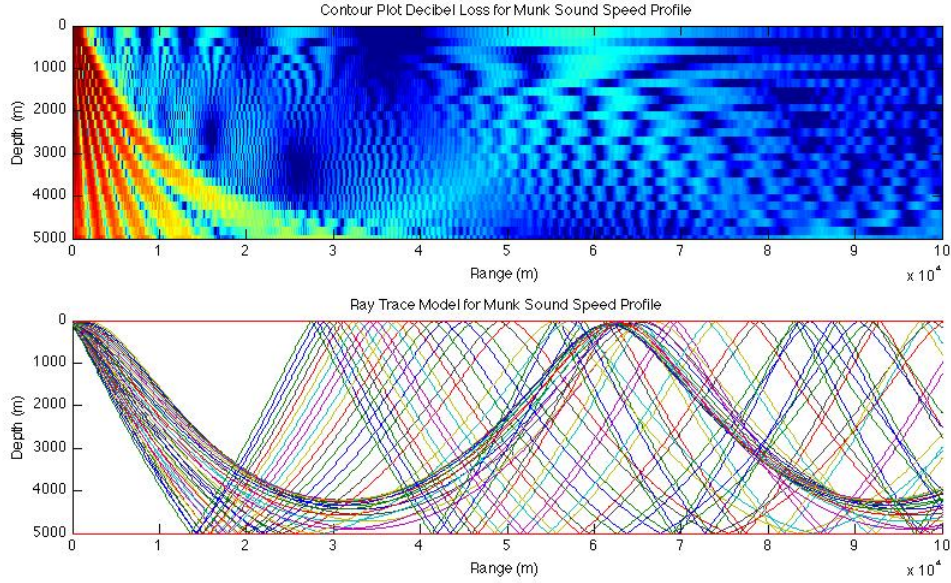
Figure 3.2: Spectral Model TL Plot and ray-trace results for a deepwater Munk sound speed profile and a surface source.

Normal Mode propagation models work by approximating the solution to the wave equation as the sum of a series of discrete normalized modes. The modes shown in Figure 3.3 can be represented by equation 3.9.

$$\psi_m = \sqrt{\frac{2\rho}{D}} \sin k_{zm} z \qquad (3.9)$$

The acoustic pressure in a given point in the waveguide is given by the sum of each mode with the Green's function at that point in the medium with a source term and a normalization factor as shown in equation 3.10.

$$p(r,z) = \frac{i}{4\rho(z_s)} \sum \psi_m(z_s)\psi_m(z) H_0^{(1)} k_{rm} r - \int_{C_{EJP}} \qquad (3.10)$$

By summing these mode shape functions, it is possible to approximate the intensity of the acoustic field at any point in the water column. A transmission loss plot like the one in Figure 3.4 can be generated.

Normal mode propagation models are considered the workhorse of propagation models in that they are sufficient for most purposes. Normal mode models are highly computationally efficient in that the mode shape functions only need to
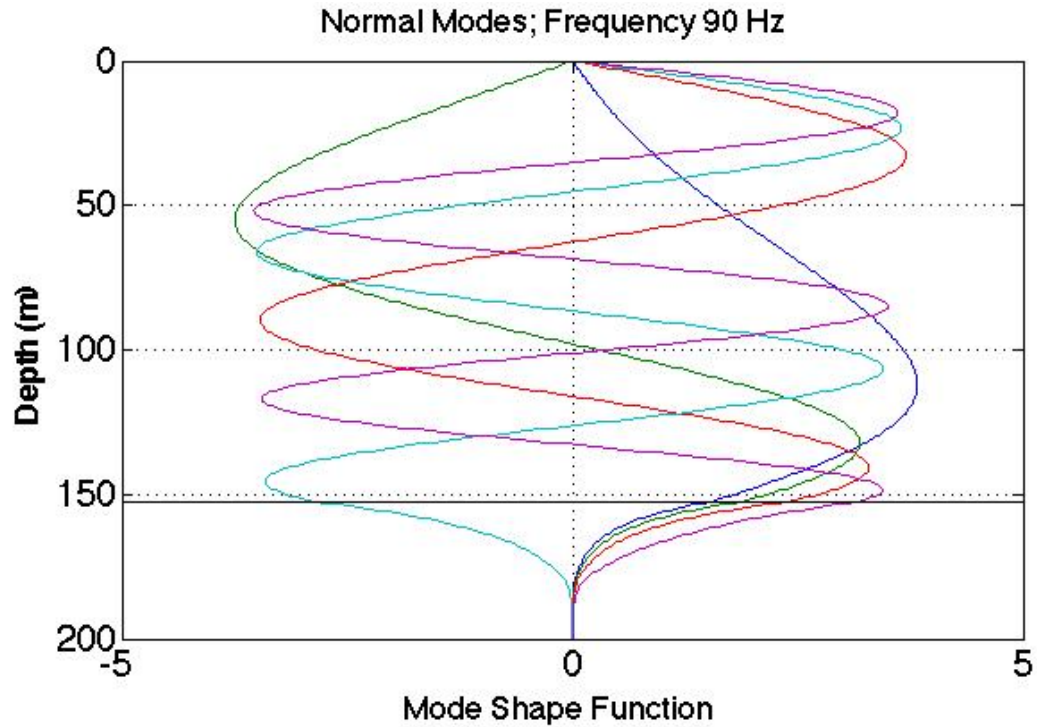
Figure 3.3: Normal Modes as a function of depth.
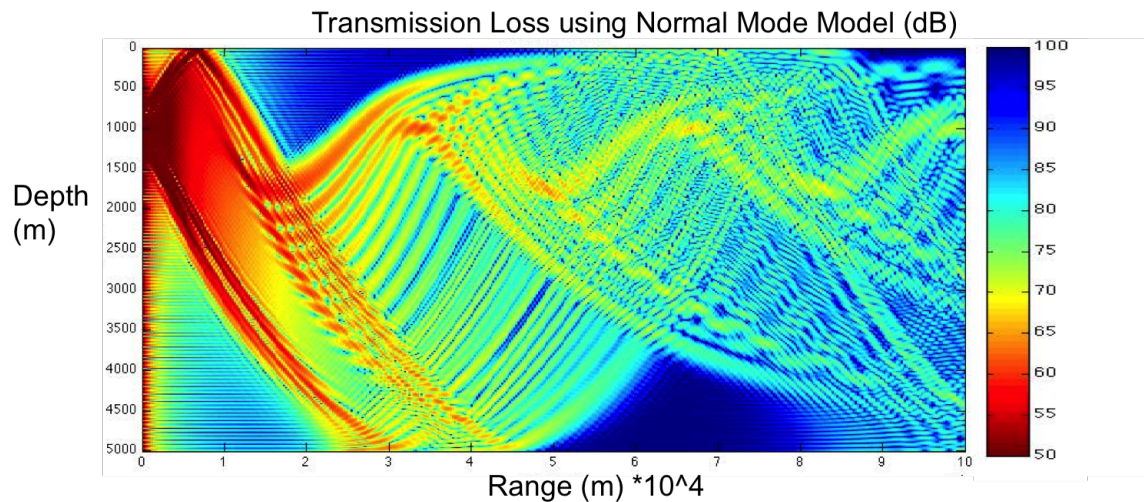
Figure 3.4: Normal Mode Transmission Loss Plot for deepwater Munk sound speed profile with a source depth at 1000 m.

be calculated once for a given acoustic environment. Normal mode models are not considered good approximations for near-field propagation simulations, as it takes

time for the normal modes to build up to the point where they can approximate the full field. Normal mode models are not very effective at dealing with range dependent environments; i.e. environments when the depth, bottom characteristics, or sound speed profiles change with horizontal distance, as for each new environment, whole new sets of modes need to be calculated, eliminating the computational savings that made the normal mode model a desirable choice to begin with. For range dependent cases, Parabolic Equation models are far more effective and computationally efficient. Nevertheless, because of their computational efficiency, and high degree of accuracy in the far-field, normal mode propagation models are often used in ocean acoustic applications such as Matched Field Processing.

Parabolic Equation based propagation models are the most popular solutions to the wave equation in ocean acoustics for range dependent cases. The wave equation is second order in range and depth. Representing the solution as elliptic equations with boundary conditions is difficult, but if the boundary conditions are approximated the wave equation can be represented instead by a parabolic equation with a set of initial conditions and a 'marching algorithm' to propagate it forward in space. The original application of the Parabolic equation in ocean acoustics implemented in the 1970s used a split step algorithm to propagate the equation forward, and an antisymmetric starter function to account for surface boundary conditions [9]. There are a variety of versions of parabolic equation solutions available now, using slight modifications to the marching algorithm, differing treatment of boundary conditions, and plethora of different starter functions but they are all based on the same theory. In parabolic equation propagation models, the solution to equation 3.13 can be used to represent the pressure field for a given depth and range as shown in equation 3.11 using the Hankel function defined in equation 3.12.

$$p(r, z) = \psi(r, z) H_0^{(1)} k_0 r \tag{3.11}$$

$$H_0^{(1)} k_0 r = \sqrt{\frac{2}{\pi k_0 r}} e^{(k_0 r - \frac{\pi}{4})} \tag{3.12}$$
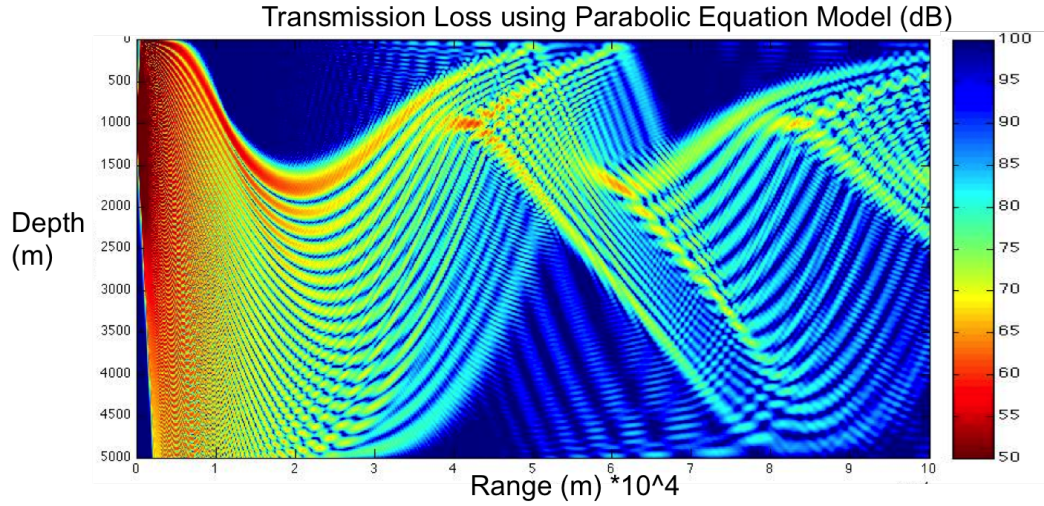
Figure 3.5: Parabolic Equation propagation model Transmission Loss Plot for deepwater Munk sound speed profile with a source depth at 1000 m.

$$2ik_0\frac{\delta\psi}{\delta r} + \frac{\delta^2\psi}{\delta z^2} + k_0^2(n^2 - 1)\psi = 0 \tag{3.13}$$

Parabolic equations models are highly computationally efficient, they deal with range dependent environments better than perhaps any other method, but they are not good near-field approximations for the wave equation, as in the near field the results will inevitably just resemble the starter function. Figure 3.5 shows the transmission loss results for a parabolic equation model for the same environment used for the normal mode model seen above.

Matched Field Processing is a source localization technique that uses one of the above propagation models to generate replica fields on an array of sensors for a source at every possible location in a grid, then compares each of these replica signals to the actual signal received across the array using one of the beamforming methods discussed in the previous section (Bartlett, MVDR, or WNC). The source position in the grid that generates the field across the array that most closely correlates to the received signal on the array must then be the location of the unknown source. The idea is very simple, and under certain circumstances the method is highly effective. Figure 3.6 shows Matched Field Processor output for an attempt at localizing an active acoustic source approximately 50 meters deep,
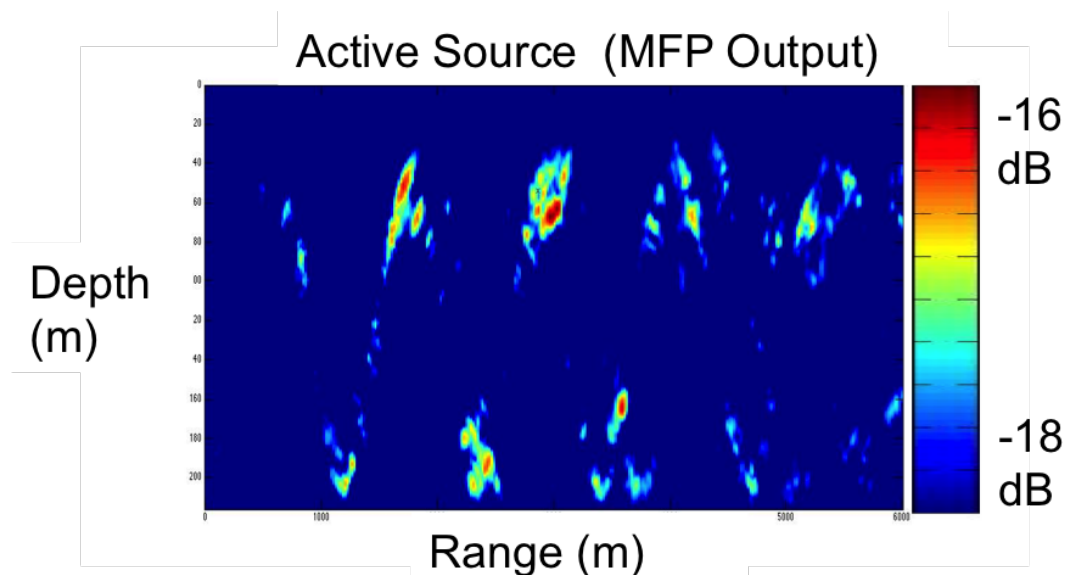
Figure 3.6: MFP results using a normal mode propagation model and linear Bartlett beamformer to localize a towed active source 50 m deep, 3 km from a moored vertical array, during the Swell_Ex 96 acoustic experiment.

approximately 3 km away from a moored vertical array during the Swell-Ex 96 ocean acoustic experiment. The acoustic environment for this experiment was well characterized, the bottom properties well-known, and the environment, to first order, could be approximated as range independent. In short, the circumstances were nearly ideal for matched field processing. A normal mode model was used to generate replica fields, and a Bartlett beamformer was used to compare the replica library to the received signal. This was done for several discrete frequencies and the resulting ambiguity surfaces were summed incoherently and geometrically. The results are shown below, and you can see that the red dot is very close to the black 'x' representing the true location of the source. In this case, MFP effectively localized the source.

In the 1990s MFP showed a great deal of promise due to results such as the one above. Unfortunately the method does not always work, and in fact breaks down in most real-world ocean conditions. The primary limitation of MFP as a source localization method is our ability to sufficiently model the acoustic environment. Rarely do we have enough information about the sound speed profile and bottom characteristics to construct our propagation models with sufficient ac-

curacy to localize an acoustic source in the water column consistently. The more complicated the acoustic environment, the more this method breaks down. Complicated sediment layering structure, scattering from internal waves, other physical oceanographic perturbations, and uneven bottom characteristics all cause traditional matched field processing to break down. Spatial and temporal variations in the acoustic environment are especially hard to account for in MFP methods. Due to our inability to model acoustic propagation in the ocean environment with sufficient accuracy, MFP has largely been abandoned by the field as a source localization method. The fundamental flaw in the method is the reliance on the operators' ability to accurately model the acoustic environment using one of the aforementioned propagation models. If one could eliminate the need for modeling, the fundamental theory of MFP could still be applied to localizing acoustic radiators in an ocean environment.

3.2 Source Localization Using Measured Correlation Replica Fields from Sources of Opportunity

This section describes a proposed method of localizing acoustic sources that is similar to matched field processing, but does not rely on one's ability to model the acoustic environment. Instead measured replica fields taken from historical data libraries are used in place of modeled replica fields for comparison with data received across the array. The method discussed here differs from previous source localization techniques in three critical ways. The first difference between this method and previous studies is the use of measured replica fields rather than modeled replicas. In other words, the library the data is compared to is made up of correlation values determined from historical data associated with times when sources were located in certain grid points [10]. The inclusion of sources of opportunity is also unique. In previous studies that utilized measured replica fields for source localization, towed acoustic sources were used. No active sources are used

in this study; all acoustic sources are sources of opportunity; in this case, ships. The final difference between this study and previous studies is that this study utilizes the correlation of the signal received across hydrophones separated horizontally, such as those on two horizontally separated vertical arrays rather than the signal itself as the library for comparison and the signal to compare. The use of correlation vectors in place of the actual acoustic signal for differencing the library of replicas from the data, is the fact that ships as sources of opportunity all possess different spectral characteristics, and a comparison of the actual acoustic signal would be meaningless; but the cross-correlation of the signals on two horizontally separated arrays is based on the arrival structure, and is therefore frequency independent, meaning it can be used to compare signals coming from sources with different frequency content.

In this study, we make use of Automatic Identification System (AIS) ship tracking data in order to build the library of correlation vectors. Essentially vectors of the correlation between two vertical arrays were saved when ships were located on certain grid points, and were associated with those grid points. Then when a new signal was received, the correlation vector of the signal across the same two hydrophones was correlated with the library of correlation vectors and the grid point with the correlation value that most closely correlated with the data correlation vector was taken to be the location of the source in the new dataset.

This study uses acoustic data gathered during the Office of Naval Research supported field Experiment, Noise 09. Noise 09 was a ten day experiment that involved deploying 4 vertical line arrays (VLAs), with 16 elements each with the configuration illustrated in Figure 3.8. VLAs 1, 2, 3, and 4 were deployed approximately 15 km offshore of San Diego, CA, spaced 500m, 1000m, and 1500m apart respectively. The depth of water in the experiment area was approximately 150m. The array positions are illustrated in Figure 3.7.

The acoustic environment for this study region is well characterized. A total of 9 CTD casts were completed surrounding the array positions and there is good historical and climatological physical oceanographic data available for this area. These data are sufficient to estimate the sound speed profile characteristics
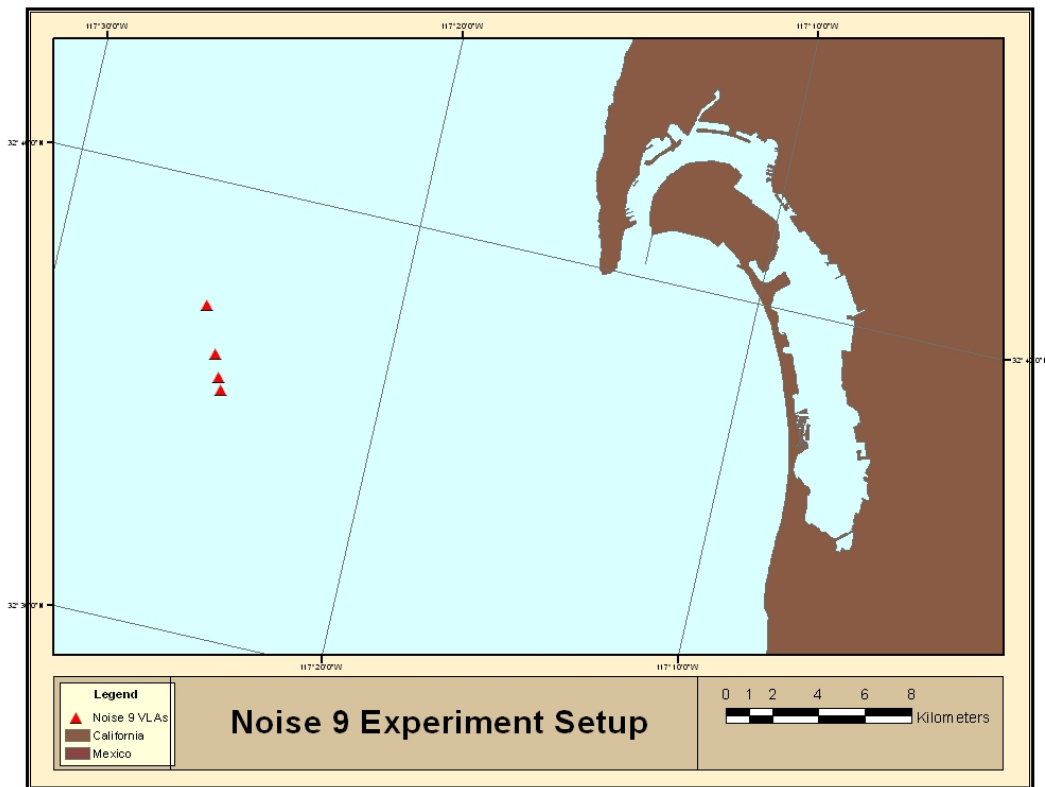
Figure 3.7: Noise 09 Sensor Positions

of the region surrounding the arrays. The seafloor is also well-studied and has been characterized sufficiently for modeling purposes here. High-resolution bathymetry data for this region is also available. Figures 3.9 and 3.10illustrate the Sound Speed Profile, Density, and Attenuation profile used in the model to simulate the Noise 09 acoustic environment. Understanding this environment is important for selecting regions where this method would be expected to work, and for constructing a model for simulating acoustic signals on the array.

As discussed in the introduction section of this chapter, traditional methods of passive source localization such as Matched Field Processing are limited by one's ability to accurately model the acoustic environment, and thus ultimately fail; this technique is designed to eliminate the need for modeling. This technique builds a library of 'replica fields' not from simulated data from a model, but from

RAVA Deployment For NOISE 09

Recovery Buoy
(Radio Beacon, Flasher
and Radar Reflector)

Distributed Floats

Lifting Eye

5m

3m

Low Drag Float   0.7m

Tiltmeter
Hydrophone # 16
Hydrophone # 15

1m

1m

150m

20m

27m

Lift Eye

Hydrophone # 2
Hydrophone # 1

1m

1m

Recording Package

Dual Acoustic Release   6m

Steel Ring

Anchor
(1000 lbs.)

3.5m

2.5m

1/28/09
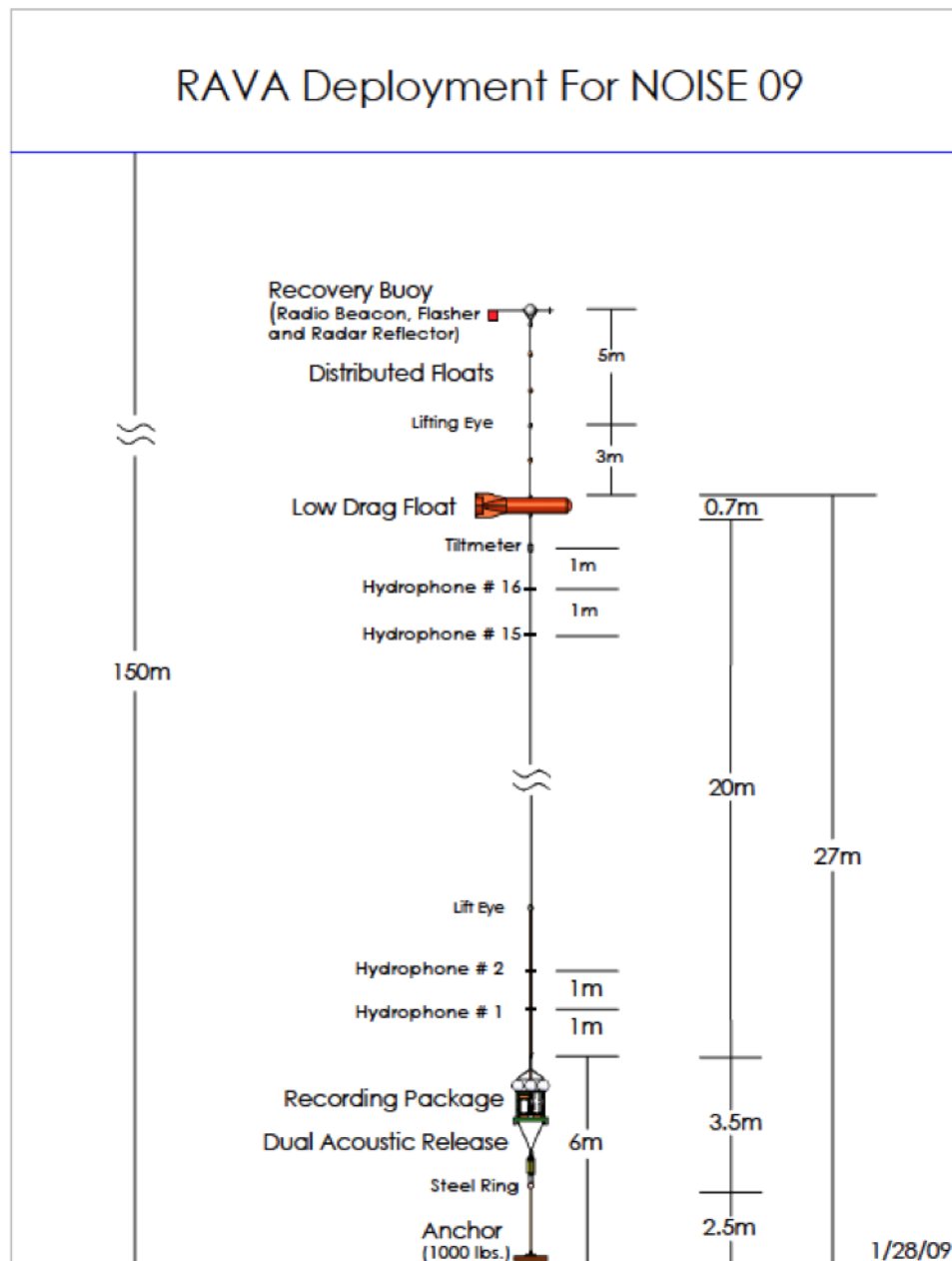
Figure 3.8: Noise 09 Array Setup

observational real-world data. These 'measured replica fields' are generated when an acoustic source is in a certain position. The acoustic signal on two hydrophones are recorded and associated with the latitude and longitude of the radiator at the time of recording. These values are used to populate an entire grid of replica
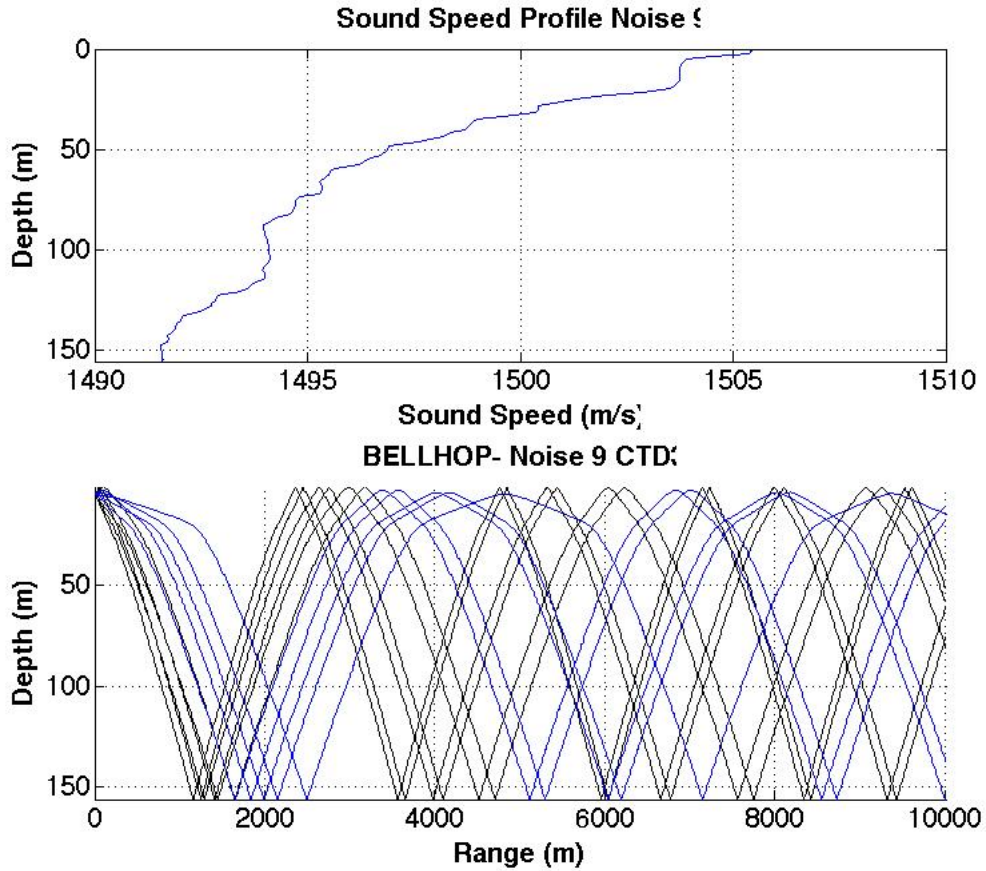
Figure 3.9: Sound Speed Profile and output of Bellhop ray-trace model for Noise 09 Acoustic Environment.

fields. As this is a passive technique, a towed active acoustic source is not used to generate the measured replica fields. This would be impractical, as it would need to be continuously redone as the ocean environment changes, and also completely eliminates the point of a passive source localization technique, if it relies on active techniques to build the library. Instead, we utilize acoustic 'sources of opportunity' in order to generate our measured replica fields. In the case of this study, we use ships as sources of opportunity. This is logical as the sources we are likely attempting to localize are also ships.

The challenge with using ships as sources of opportunity is that each ship sounds different. Inherently sources with differing spectral characteristics will not correlate and any attempt to difference replica and data vectors will break down
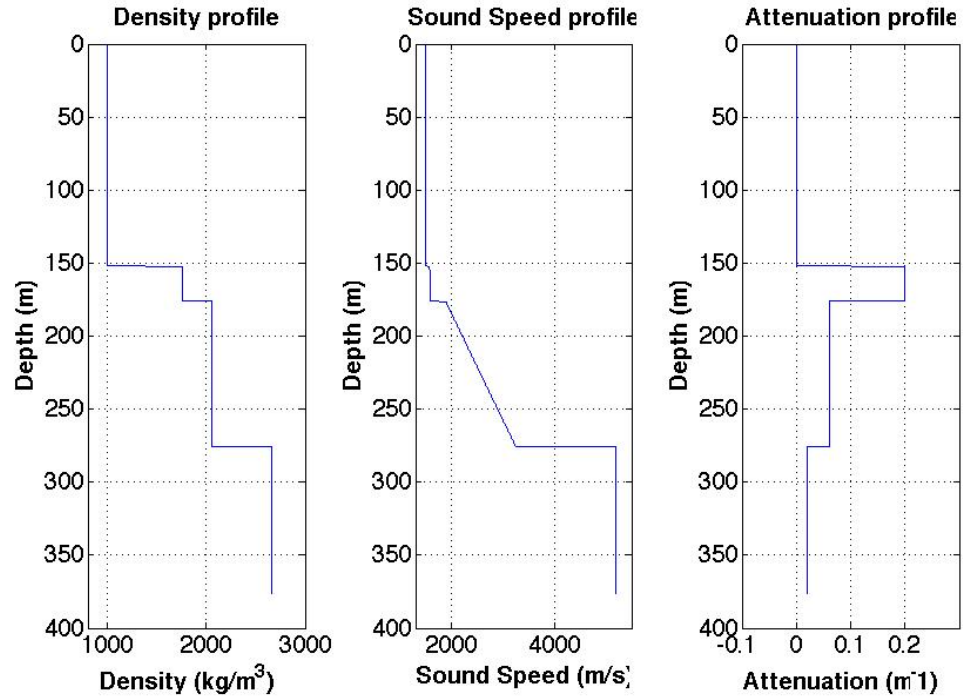
Figure 3.10: Noise 09 Acoustic Environment.

for ships with differing spectra. It is helpful to think of the signal received on an acoustic array as the convolution of the signal generated by an acoustic radiator and a transfer function, or Green's function, associated with the ocean waveguide between source and receiver. This is illustrated conceptually in equation 3.14 where s represents the acoustic signal of the ship at the source location, f represents the transfer function of the waveguide, and d represents the data actually received on the array.

$$s(t) * f(t) \to d(t) \tag{3.14}$$

In our case, the acoustic signal generated by the radiator will be different between ships, as each ship has unique spectral characteristics, but the transfer function will be the same for one ship in a given location and any other in that same location. Figure 3.11 and 3.12 show spectrograms of acoustic signals generated by two different ships. It is clear that if one were to attempt to difference the time domain signals from these two ships the results would not be meaningful, so
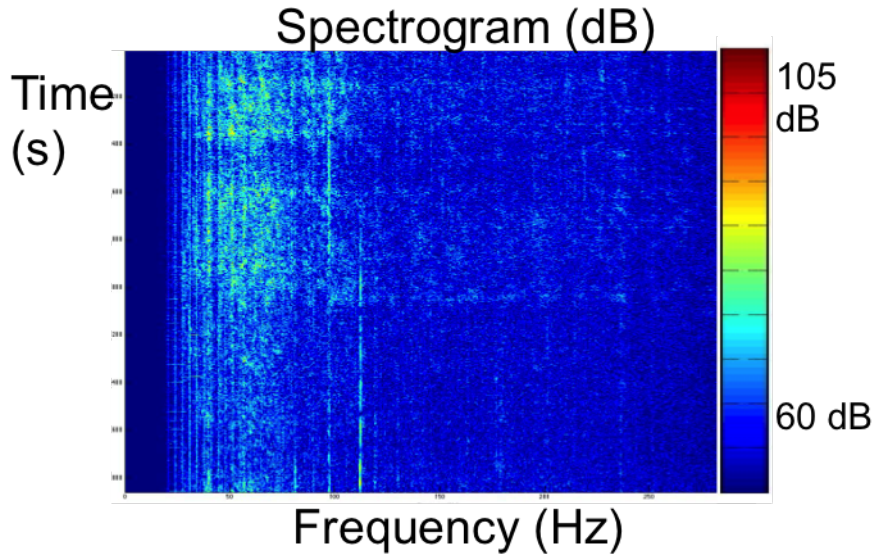
Figure 3.11: Time evolving power spectrum (Spectrogram) from one ship. This ship was the ship used to populate the library of replica correlation vectors.

comparing the acoustic signal from one, with the other, would not result in source localization. The difference between the signals would be due to the difference in spectral characteristics of the two ships, rather than the location of the source. So it is the Green's function that gives each position on our grid uniqueness and allows us to localize a source. The signal from the ship itself can be thought of as a nuisance parameter, and by using the cross-correlation of the signal between two elements, instead of the acoustic signal itself, we account for that, and eliminate the nuisance parameter. This method relies upon the uniqueness of the transfer function between different source locations carrying over into the cross-correlation vector with enough substance to uniquely identify signals generated in different locations.

In order to account for the incoherence between acoustic radiators with differing spectral characteristics, we eliminate all phase information by cross correlating the signals on two elements separated by some arbitrary horizontal distance. This process is illustrated in Figure 3.13, which shows a ship, the signal received on two hydrophones on adjacent arrays, and the cross-correlation of the two signals. This cross-correlation vector is then saved associated with the latitude and
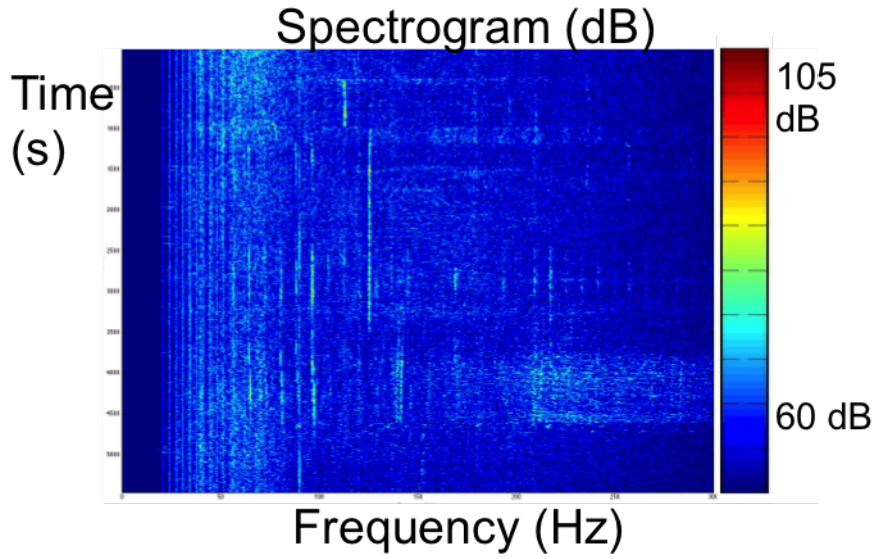
Figure 3.12: Time evolving power spectrum (Spectrogram) from another ship. This particular ship was the ship that was eventually localized using the library created using the signal from a different ship with different spectral characteristics.

longitude of the acoustic radiator that generated the correlated signals, and is used as the library replica field. Correlation vectors are used for comparison between library replicas and data instead of raw acoustic signals in order to account for the different spectral structures of different ships.

Cross-correlation is a measure of how similar two time series are in terms of a time delay applied to one or the other of the signals. Mathematically, it is the sliding inner-product of the two time series. It is equivalent to the convolution of one signal with the time-reversed version of the other signal. In the time domain a cross-correlation can be computed as shown in equation 3.15and 3.16.

$$(f \star g)(\tau) \equiv \int f^*(t)g(t+\tau)dt \tag{3.15}$$

$$f \star g \equiv f^*(-t) * g(t) \tag{3.16}$$

This means that in the frequency domain a cross-correlation can be expressed as the multiplication of one signal by the complex conjugate of the other 3.17.

$$f(t) \star g(t) = ifft(F(\omega)G(\omega)^*) \tag{3.17}$$

Once a grid of library correlation replicas has been generated, you can compare these correlation vectors to the 'data' correlation vectors, referring to the cross-correlation of the acoustic signals on the two hydrophones in the presence of an unknown acoustic radiator, which we will call the 'event' correlation vector. Least squares differencing or cross-correlation of the two cross-correlation vectors can be used for comparison of the library replicas to the event data. The process is illustrated in Figure 3.13.

The following discussion walks through the process, starting with the creation of the library of replica correlation vectors, moving through the calculation of the event correlation vectors, and finally describing the differencing method of comparing the event correlation vector with the library of correlation vectors. In this embodiment of the method, for simplicity, we use only one element on each of two vertical arrays, at approximately the same depth, separated by approximately 500 meters. The first step was to select a grid to use to create a library, determine which ships cross through that grid, and download the ship track data (time, position) for each ship while it crosses through the grid; then download the acoustic data for these same time periods. Ultimately, we will associate cross-correlations of the acoustic signals across two array elements with the position that a ship was in, when those time series were generated. This will be our library of measured cross-correlation replica fields. We start with the time series on each element, X1(t) and X2(t), shown in the below equations 3.18,3.19, and 3.20. Each time series is filtered using a standard 4th order digital Butterworth bandpass filter selecting the frequency content between 20 and 300 Hz to focus on the area of the spectrum dominated by shipping noise. The filtered time series are decimated for computational savings, as the original sample frequency of 25 kHz far exceeded what we require for these purposes, then Fourier transformed and one is multiplied by the complex conjugate of the other in order to compute the cross-correlation vector of the two time series. Taking the inverse Fourier transform of the resulting vector results in the cross-correlation in the time domain 3.21. These time-domain
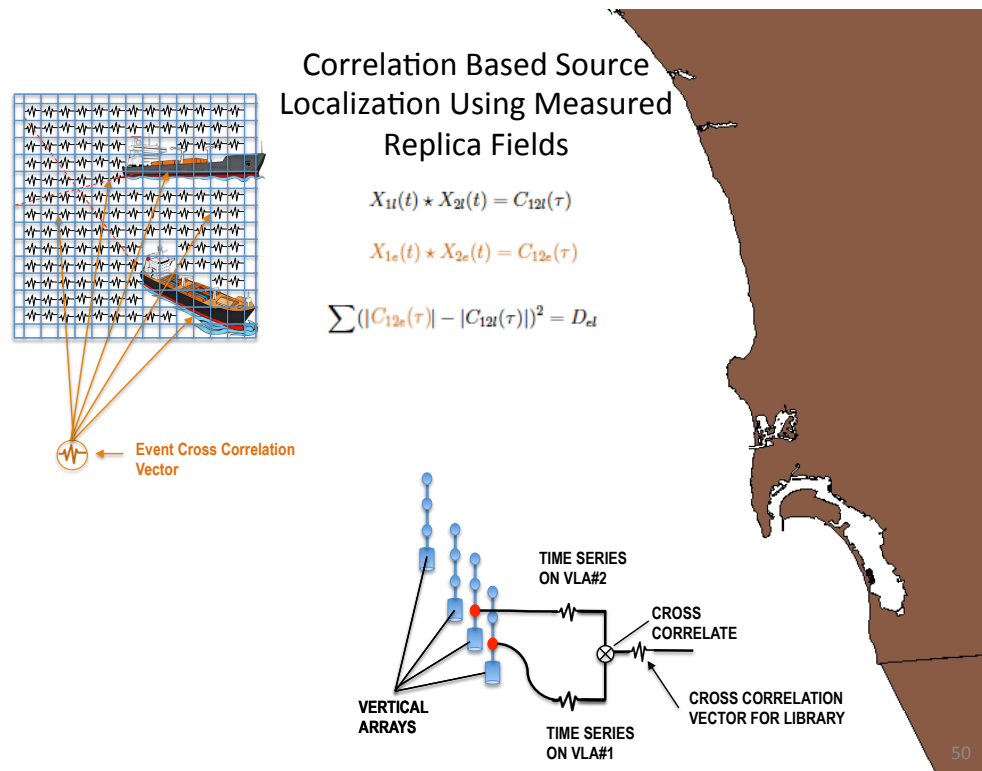
Figure 3.13: An illustration of the theory behind this source localization method. There are four vertical arrays approximately 15 km offshore of San Diego (as in Noise 09). A grid is constructed; the time signal on each of two hydrophones on adjacent arrays are cross correlated, and the resulting time domain cross-correlation vector is saved associated with the latitude and longitude of the ship that created the signal at the time of recording. Ultimately the goal is to populate the entire grid with correlation vectors (measured replicas) from when ships were in each position in the grid. This library of measured replica correlation vectors is then compared to the cross-correlation of the time signal on the two elements in the presence of an unknown acoustic radiator, and whichever library vector most closely correlated to the event vector must then be the location of the unknown acoustic radiator.

cross-correlation vectors are saved associated with latitude and longitude of the ship that generated the signals. This is our library of replica correlation fields.

$$X_1(t) \rightarrow Filter \rightarrow FFT \rightarrow X_1(\omega) \tag{3.18}$$

$$X_2(t) \rightarrow Filter \rightarrow FFT \rightarrow X_2(\omega) \tag{3.19}$$

$$X_1(\omega)X_2(\omega)^* \rightarrow C_{12l}(\omega) \tag{3.20}$$

$$C_{12l}(\tau) = ifft(C_{12l}(\omega)) \tag{3.21}$$

Once we have a library of cross-correlation vectors all that is left is to compare these correlation vectors to the correlation vector generated for the event data as shown in equations 3.22, 3.23, 3.24, and 3.25. The acoustic signals on the two elements during the event involving the unknown acoustic radiator are cross correlated and this cross-correlation vector is compared to the library of cross-correlation vectors associated with latitude and longitude using either least squares differencing or another cross-correlation.

$$X_{1e}(t) \rightarrow Filter \rightarrow FFT \rightarrow X_{1e}(\omega) \tag{3.22}$$

$$X_{2e}(t) \rightarrow Filter \rightarrow FFT \rightarrow X_{2e}(\omega) \tag{3.23}$$

$$X_{1e}(\omega)X_{2e}(\omega)^* \rightarrow C_{12e}(\omega) \tag{3.24}$$

$$C_{12e}(\tau) = ifft(C_{12e}(\omega)) \tag{3.25}$$

In the time domain this can be done directly with a cross-correlation operation as in equations 3.26 and 3.27.

$$X_{1l}(t) \star X_{2l}(t) = C_{12l}(\tau) \tag{3.26}$$

$$X_{1e}(t) \star X_{2e}(t) = C_{12e}(\tau) \tag{3.27}$$

The resulting event cross-correlation vector is compared to the library of correlation vectors using least squares differencing or cross-correlation as in equations 3.28 and 3.29.

$$C_l(\tau) \star C_e(\tau) = C_{el} \tag{3.28}$$

$$\sum (|C_{12e}(\tau)| - |C_{12l}(\tau)|)^2 = D_{el} \tag{3.29}$$

Now that the theory has been developed, what remains is to test the theory using simulations then validate the theory using experimental data.

Chapter 3, in part is currently being prepared for submission for publication of the material. Verlinden, C.M.A.; Kuperman, W.A. The thesis author was the primary investigator and author of this material. Dr. William Kuperman, the chair of the committee, is the co-author.

Chapter 4

Simulations

The first step in order to test the theory described in the above sections is to use simulated acoustic data generated using acoustic propagation models for the creation of the library of replicas, and use another model to generate the 'data' acoustic signal. The purpose of testing the theory first using a model is to check the validity of the theory in simulated conditions; experiment with resolution limitations and optimal grid sizes; experiment with performance in different Signal to Noise Ratio (SNR) conditions; and to test the mechanics of the programs in controlled circumstances before applying them to real acoustic data sets. I used a normal mode based propagation model as described in the previous section using the following approximation for the wave equation to make my library of replicas and data signal.

$$p(r, z) = \frac{i}{4\rho(z_s)} \sum \psi_m(z_s)\psi_m(z)H_0^{(1)}k_{rm}r - \int_{C_{EJP}} \tag{4.1}$$

In order to make this an appropriate simulation for the acoustic environment I would ultimately use to test this technique with using experimental data, I used the approximate environment from the Noise 09 acoustic experiment. Figure 3.10 shows the acoustic environment (density, sound speed, and attenuation) I used in the creation of the acoustic models I used to test this method. Treating the bottom as a fluid-fluid interface with the density and sound speed characteristics of the water column and sediments in the region of the Noise 09 experiment, I
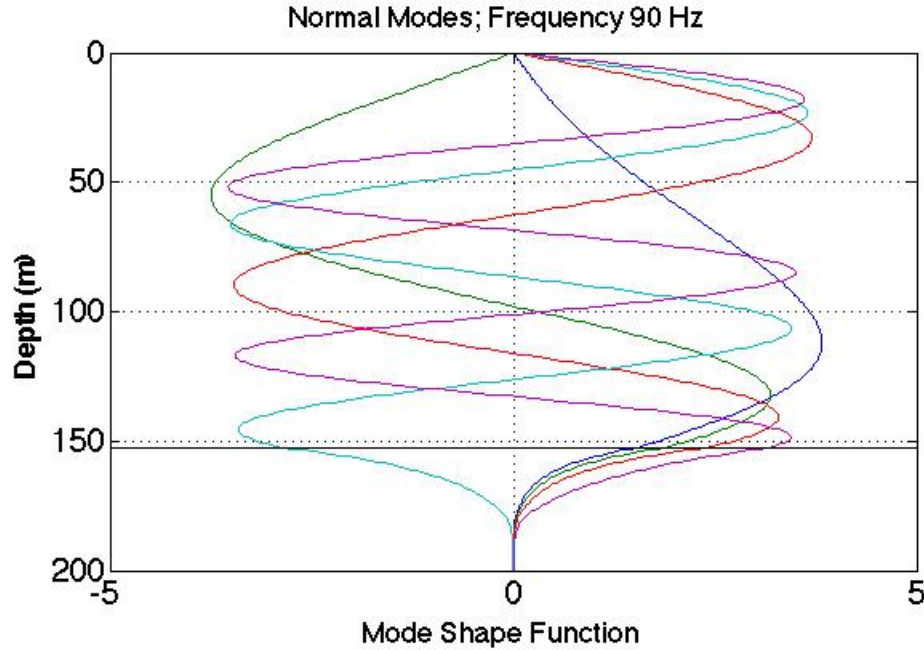
Figure 4.1: Normal Modes Used in Model (first 5 modes of 44).

estimated the modal structure of the acoustic field in this environment. Given the sound speed and waveguide characteristics illustrated in Figure 3.10, the acoustic pressure field can be expressed as the sum of 44 discrete normal modes. The first 5 normalized modes are shown in Figure 4.1.

When the normalized modes are summed with the proper weighting and Green's function applied, the acoustic pressure field anywhere in the waveguide can be approximated. Figure 4.2 shows a transmission loss plot for the Noise 09 acoustic environment.

For the first trial of my model-based simulation of this source localization method, I chose to use a range independent acoustic model. I chose a grid some distance away from the hydrophone arrays and generated simulated signals from each of the locations in the grid on the array of hydrophones. I did this in the frequency domain for several frequencies, summing the results.

Before I could test the theory using the model, I first had to do some analysis of the geometry of the problem. I needed to establish appropriate grid sizes to use for the generation of the library replicas based on the anticipated resolution
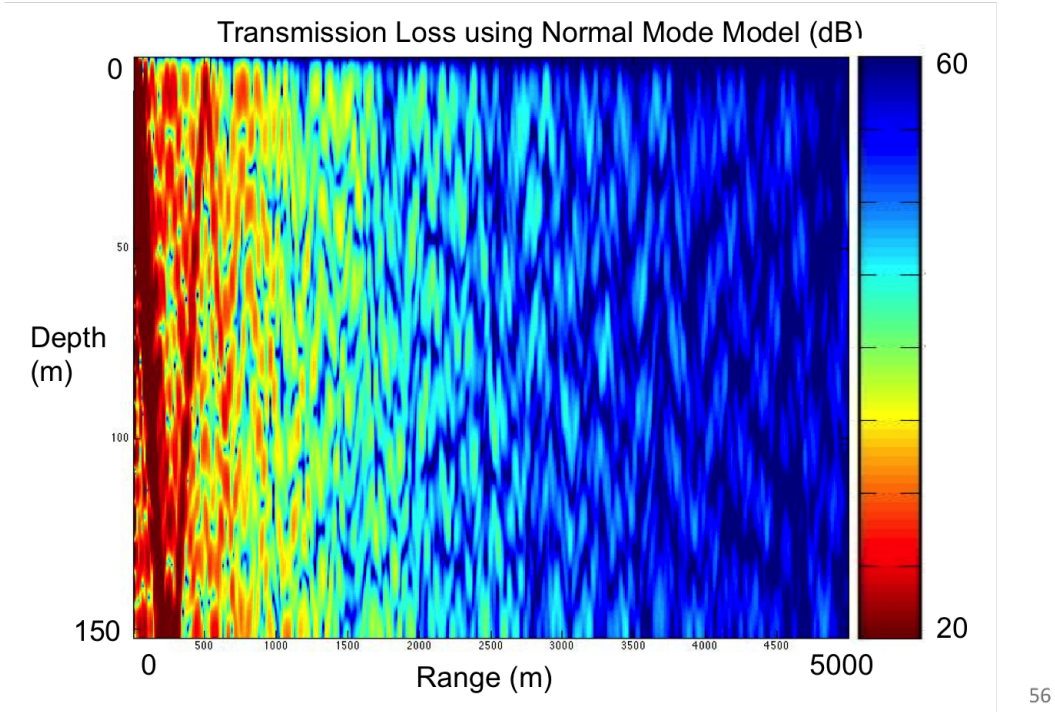
Figure 4.2: Transmission Loss plot for Noise 09 Acoustic Environment.

capabilities of the method. I chose a grid size based on the below mathematics which describe how large of spatial distance I should expect a source in a given location to be coherent over. In other words, if I used a grid size larger than this, the correlation vector in one part of a grid box would not be expected to resemble the correlation vector for a source located in a different part of the box. Equation 4.2 is the standard equation for the beam directivity of a 2 element horizontal array where d is the distance between array elements, lambda is the acoustic wavelength, and theta is the look direction.

$$B(\theta) = cos^2(\frac{\pi d}{\lambda}sin(\theta))$$

(4.2)

Typically, when constructing an array, a desired spatial sampling frequency is approximately one half the wavelength one is attempting to resolve. In this case, the elements are spaced 512 meters apart, and the wavelength of sound we are dealing with is between 5 and 75 meters. This means our array is going to experience extreme aliasing. The above beam directivity equation yields a beam
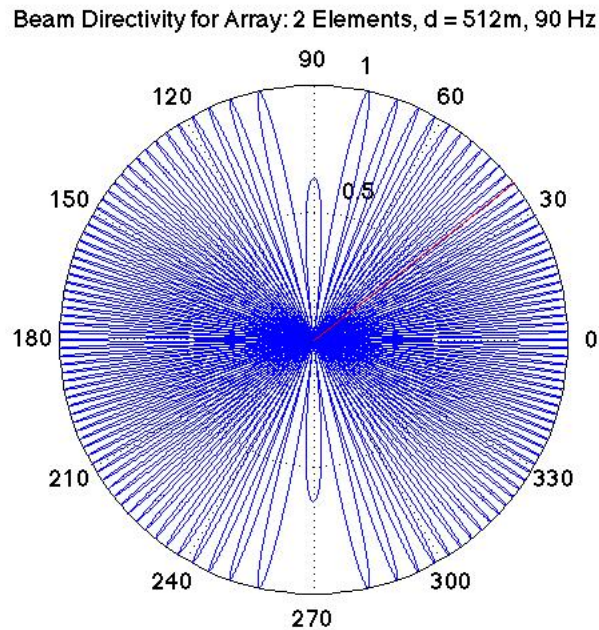
Figure 4.3: Beam Directivity for highly aliased Noise 09 array. Aperture: 512 m; Wavelength: 5-75m; Frequency: 90 Hz.

pattern showed in Figure 4.2. You can see that it is highly aliased.

Given the beam directivity shown in Figure 4.2, I know I needed to pick a grid size smaller than the lobes of the beam pattern for the highest frequency that I will be attempting to resolve. For 300 Hz, with horizontal array aperture of 512 meters, for a grid point 40 km away (the grid I am using), the lobe thickness is approximately 300 m. To be conservative I chose to use a 100 m grid size as shown in Figure 4.4. The grid I chose to use for the simulation is shown in Figure 4.5.

I also needed to conduct some analysis to determine appropriate vertical array aperture for my applications. This is based in two considerations. First of all, I needed to ensure that plane wave beamforming could appropriately be applied over the entire aperture of the array. The number of array elements that can be summed and used as a subarray for the purposes of beamforming and matched field processing is limited by the element spacing, and wavelength of signals one is attempting to beam form as described in equation 4.3[11].
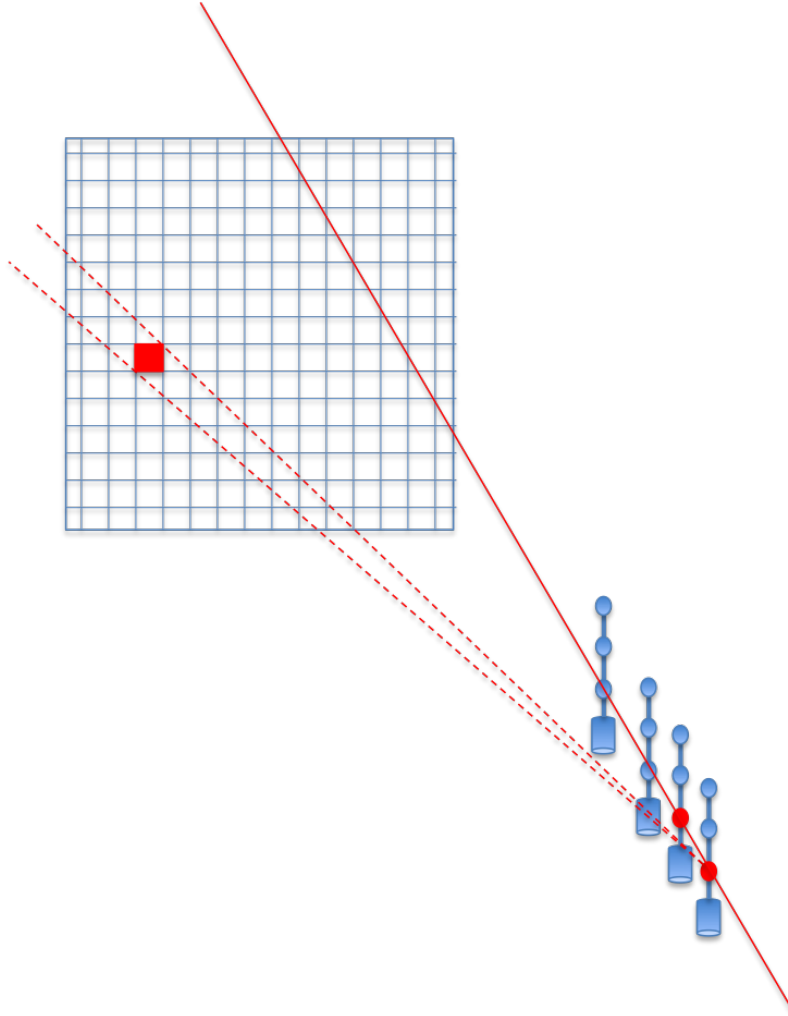
Figure 4.4: Schematic of grid size selection process. The blue towers represent the four vertical arrays used in the Noise 09 acoustic experiment, and the grid represents the library populated with ship tracks located approximately 40 km from the arrays. For a grid approximately 38 degrees off the azimuth illustrated with dotted red lines, the azimuthal resolution of the system is approximately 300 m.

$$L \leq= (\frac{\lambda_0 c_0}{2}/|\frac{dc}{dz}|)^{1/3} = c_0(2f^2|\frac{dc}{dz}|)^{-1/3} \tag{4.3}$$

For the gradient of the sound speed profile, and applicable wavelengths for this problem I could use an array with an aperture over 100 m. Given that the vertical arrays in the Noise 09 experiment are 16 element arrays with hydrophones spaced one meter apart, I will have no problem using the entire array. The other
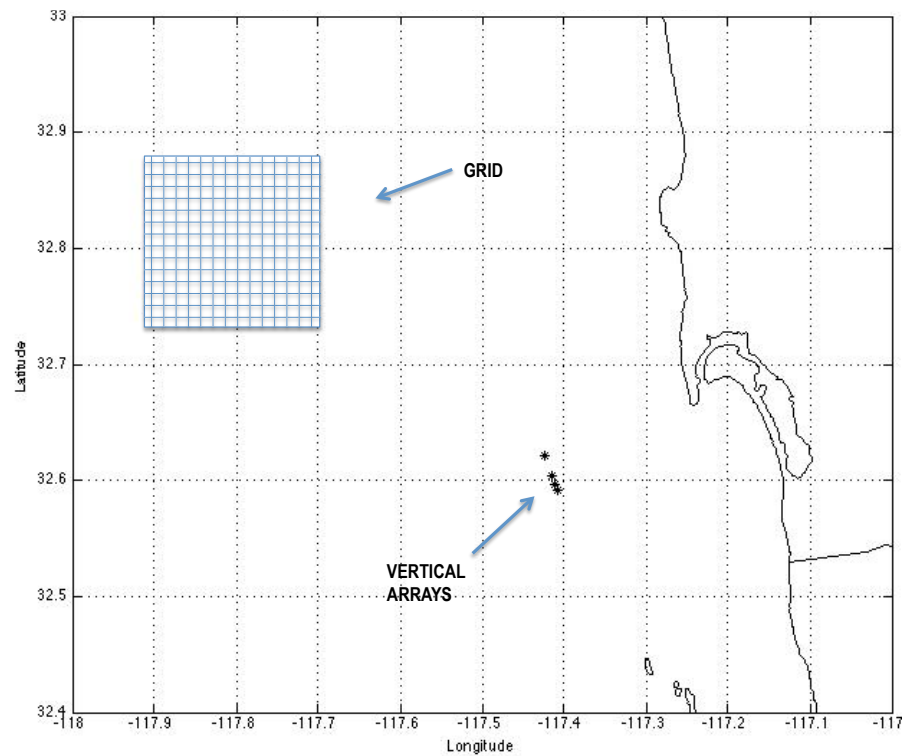
Figure 4.5: Map of Grid with Sensor Positions.

consideration that needs to be taken into account with regards to picking how many elements of the array to include in the computation of the cross-correlation vectors for this method is the ability of the array to resolve vertical directionality of incident sound waves. If I intend to sum the array elements with zero time delay applied, that is equivalent to beamforming directly along the horizontal axis. This method needs to be able to detect sub-surface contacts using replica vectors created by surface contacts, so I do not want to be able to resolve vertical directionality with the array. In other words, I want a submarine and a surface ship to look the same to the source localization method as shown in Figure 4.6. As a rule of thumb for a waveguide with a typical 21 degree critical angle, this means the array

Array Aperture
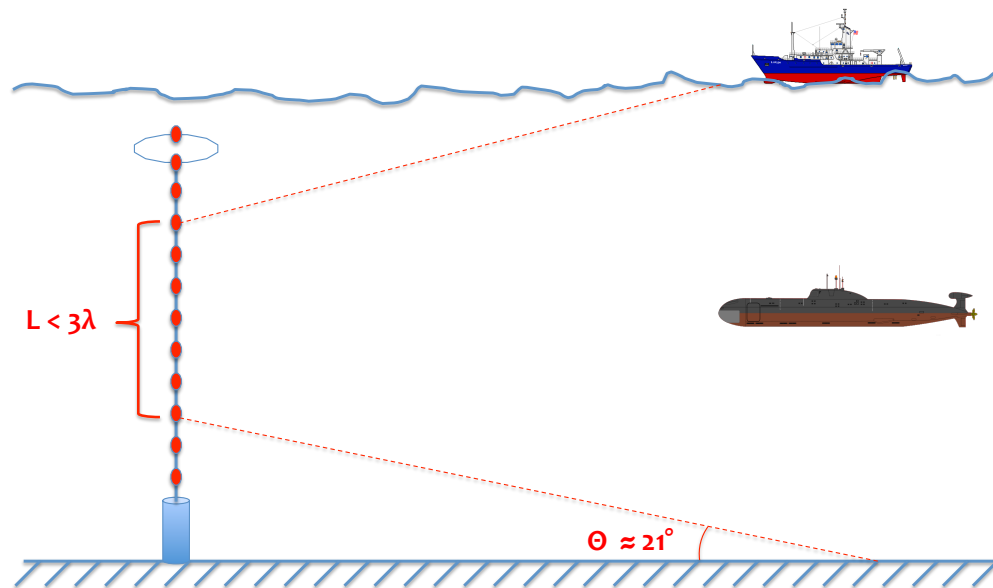
Figure 4.6: Schematic of array aperture. The array needs to not resolve vertical directionality with enough resolution to differentiate between surface and subsurface contacts. As a rule of thumb for a waveguide with a typical 21 degree critical angle, this means the array aperture must be less than 3 times the wavelength.

aperture must be less than 3 times the wavelength of the incident sound waves. For the frequencies I will be working with (20 - 300 Hz), the smallest aperture that could resolve directionality would be about 15 meters, which is about the size of the arrays used in Noise 09. This means I should be able to use the entire aperture of the array in my calculations.

Once the geometry of the problem had been established and the grid had been constructed, the grid needed to be populated with simulated replica correlations vectors. Each point on the grid was used as the source location for a simulated source, and the cross-correlation of the simulated acoustic signal received on each element in the array was recorded as a library replica value. The simulated signal

on an array element of VLA1 was cross-correlated with the simulated signal on an array element of VLA2 in the frequency domain for each of the frequencies used in the model by simply multiplying the frequency domain signal on one element by the complex conjugate of the frequency domain signal on the other element.

$$X_1(\omega)X_2(\omega)^* \rightarrow C_{12l}(\omega) \qquad (4.4)$$

The resulting cross-correlation value was saved in a grid with the associated latitude and longitude of the grid point used for the simulation that generated the signals used to create the cross-correlations. This was done for every point on the grid to populate a full library of replica correlations to use for comparison to the 'data'. Once I had a library of simulated correlation vectors, I used the same acoustic propagation model to generate a simulated 'data' acoustic signal for a simulated event involving an unknown acoustic radiator. For the first attempt, I added no noise to the system and used an exact grid point match for the location of the simulated 'unknown' acoustic radiator. Least squares differencing was used to compare the library of correlation values to the value obtained for the event as shown in equation 4.5.

$$\sum (|C_{12e}(t)| - |C_{12l}(t)|)^2 \rightarrow D_{el} \qquad (4.5)$$

Figure 4.7 shows the results of the source localization method for a single frequency (90 Hz), with zero noise. On this scale, you cannot see whether or not the source was localized, but it is useful to illustrate the side lobes associated with the aliased array beam directivity pattern shown in Figure 4.2.

Zooming in on the portion of the grid where the target source was located in Figure 4.8 we see that the source was properly localized, even at the single frequency. There are, however, significant side lobes caused by the aliased array geometry.

As one would expect, each frequency, with its own unique beam directivity pattern, aliases differently, and as a result has side lobes in different locations. Figure 4.9 shows the source localization output at four different frequencies. The source is still localized in the correct location, but the side lobes appear in different
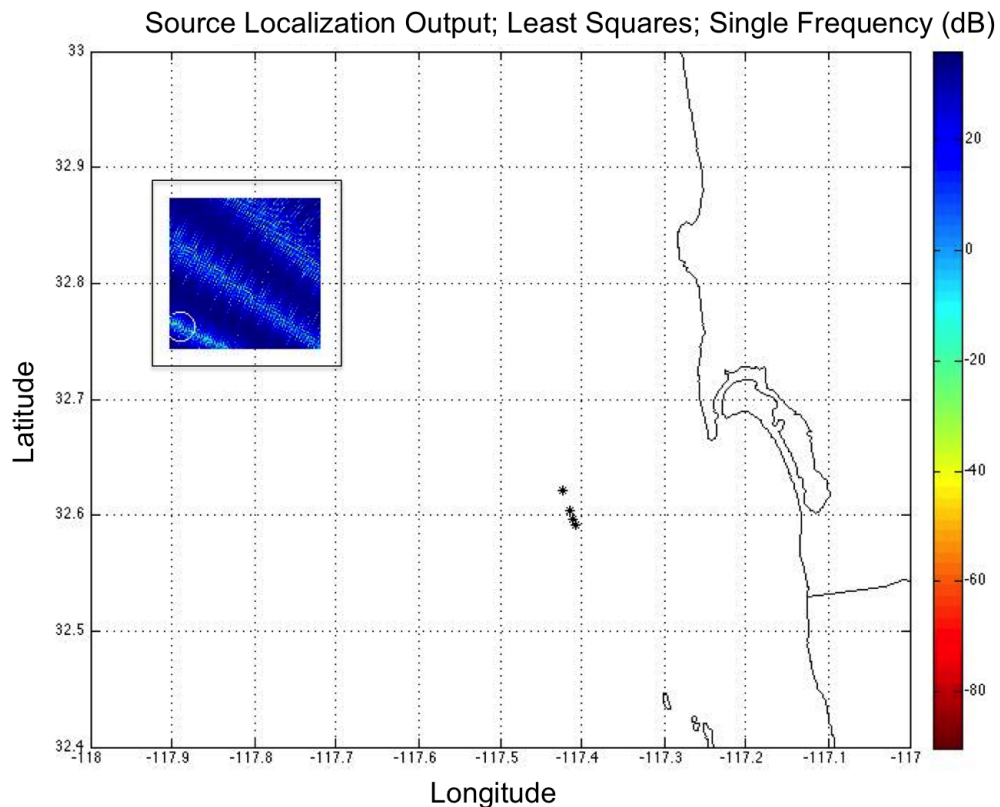
Figure 4.7: Source localization results for single frequency (90 Hz). Side lobes predicted by aliased beam directivity pattern are clearly evident.

places in each case.

Since the side lobes for each individual frequency appear in different places, it follows that if multiple frequencies are averaged together the side lobes will be reduced, while the main peak will be amplified. Figure 4.10 shows the arithmetic mean of 10 frequencies. You can see that the side lobes are significantly reduced and it is possible to see the true location of the source.

While the side lobes are significantly reduced by arithmetically summing the results of the source localizer, it is difficult to visualize the results. If the source localization method is to be interpreted by an operator looking at a display of the results, then it is useful to find a better way to display the results. Using a geometric mean, often makes the results easier to interpret visually. It is a technique commonly used in matched field processing and is essentially just averaging the

Source Localization Output; Single Frequency: 90 Hz (dB)
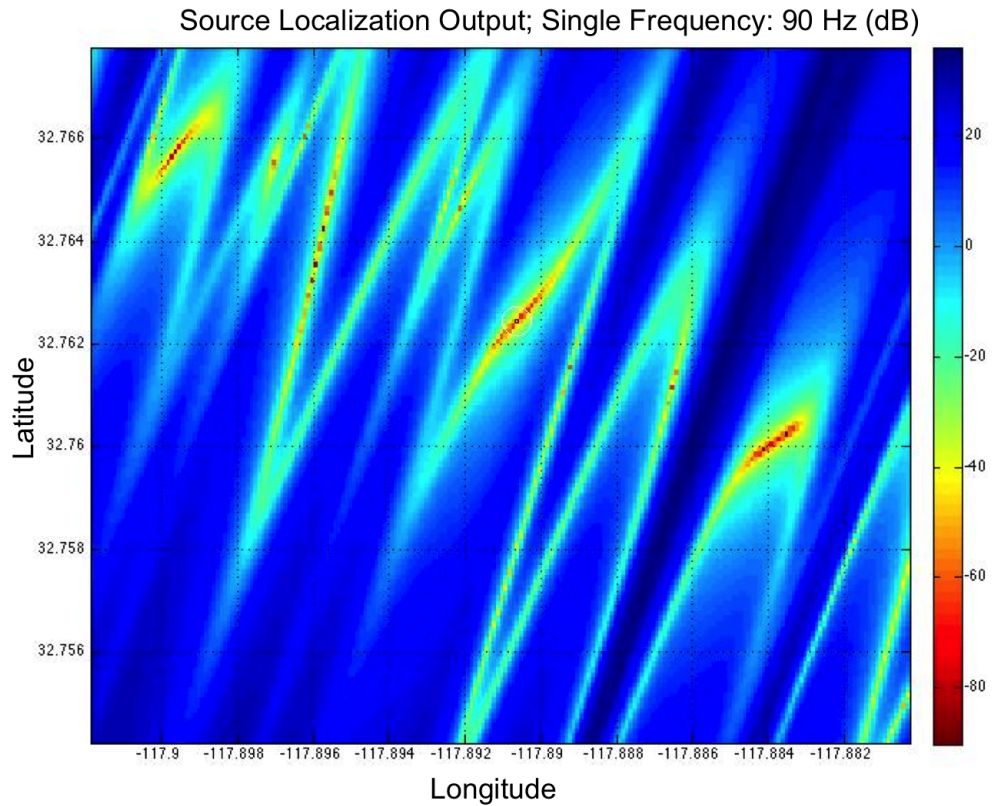
Figure 4.8: Source localization results for single frequency (90 Hz). The white circle shows the location of the source.

results in decibels. Figure 4.11 shows the geometric mean of 10 frequencies.

It is easier to visualize the localization results when the results are averaged in decibels. It is not surprising that the source was correctly located using the zero noise case, as I am essentially comparing a correlation value for the event with a library that contains an identical value. The identical value in the library will naturally be identified. All this trial shows is that individual correlation vectors generated by simulated sources in different locations can in theory be unique enough to identify sources in that location. In order to test how this method could perform under more realistic circumstances, I also performed the trial adding noise to the simulated data signal. I repeated the experiment using signal to noise ratios (SNR) of 25, 10, 5 and 1 dB. Figure 4.12 shows the results. Each Figure was generated by summing all 16 elements on the array so there is significant array
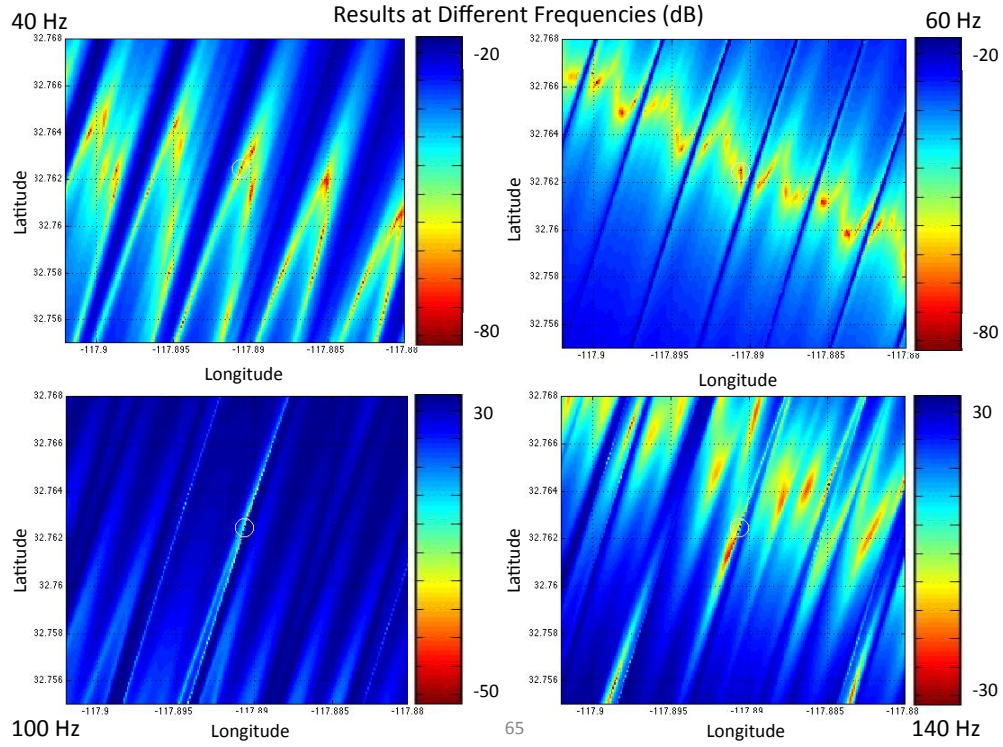
Figure 4.9: Source localization results for four different frequencies (40, 60, 100, and 140 Hz). The white circle shows the location of the source. The aliasing is different for each frequency.

gain.

In the modeled case, it is possible to localize the source in the presence of white isotropic noise, even with a signal to noise ratio as low as 1 dB, but it is unlikely the method will perform so well in the field. Often SNR is improved in open ocean acoustic experiments by summing signals collected over multiple array elements. The Noise 09 experiment had four vertical arrays each with 16 elements. I experimented with summing the signals on 4, 8, and 16 elements in a 10 dB SNR environment order to see what the impact on the resulting source localization would be for my simulated experiment.

$$S(t) = \sum s_n(t) \tag{4.6}$$
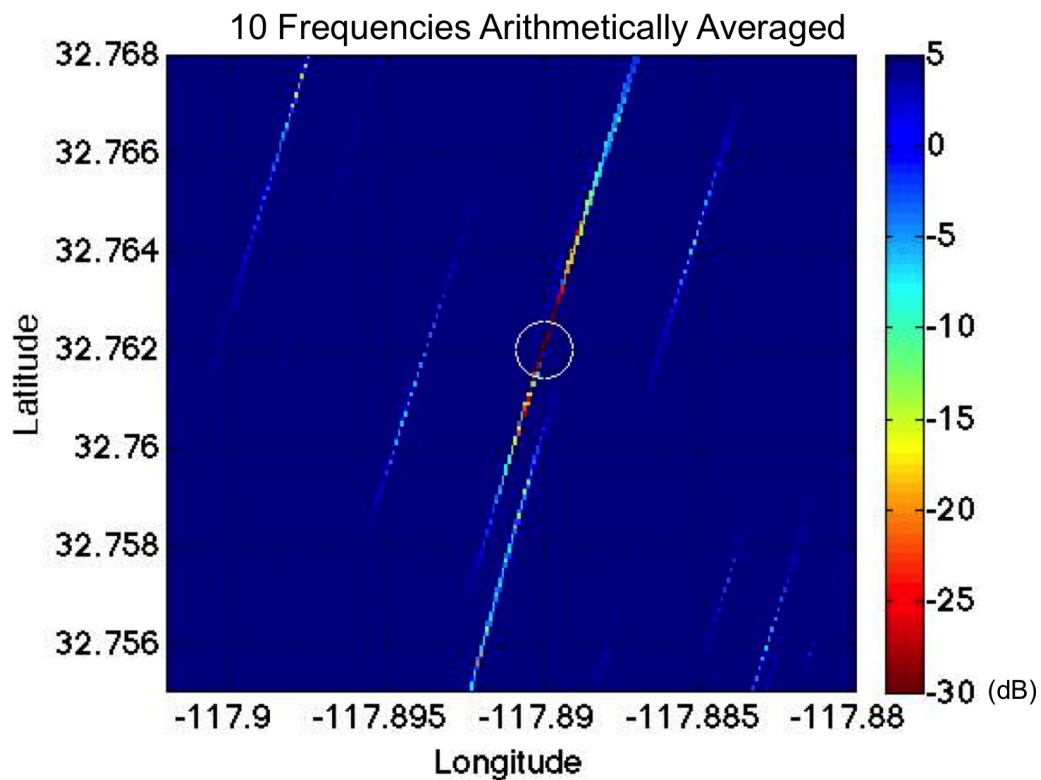
Figure 4.10: Average of Source Localization Output for 10 frequencies (Arithmetic Mean).

According to the subarray aperture analysis conducted earlier in this section, I should be able to sum 16 elements on this array and see gains in SNR, while still not resolving vertical directionality of the noise field. Figure 4.13 shows the plots of the localization surface for each of the aforementioned number of elements and in a 10 dB SNR environment.

You can see from the above plots that summing multiple elements does improve SNR. Using 8 elements, the method is able to localize the source effectively. While this is not expected to translate directly into ocean field experiments, it does suggest that this method could work in a noisy ocean environment, with the array geometry and acoustic environment characteristics of the Noise 09 experiment. The next item to test with the model was how sensitive the method is to minor perturbations in sensor locations or to sources located in locations not corresponding to exact locations used to create the replica fields. This is valuable information
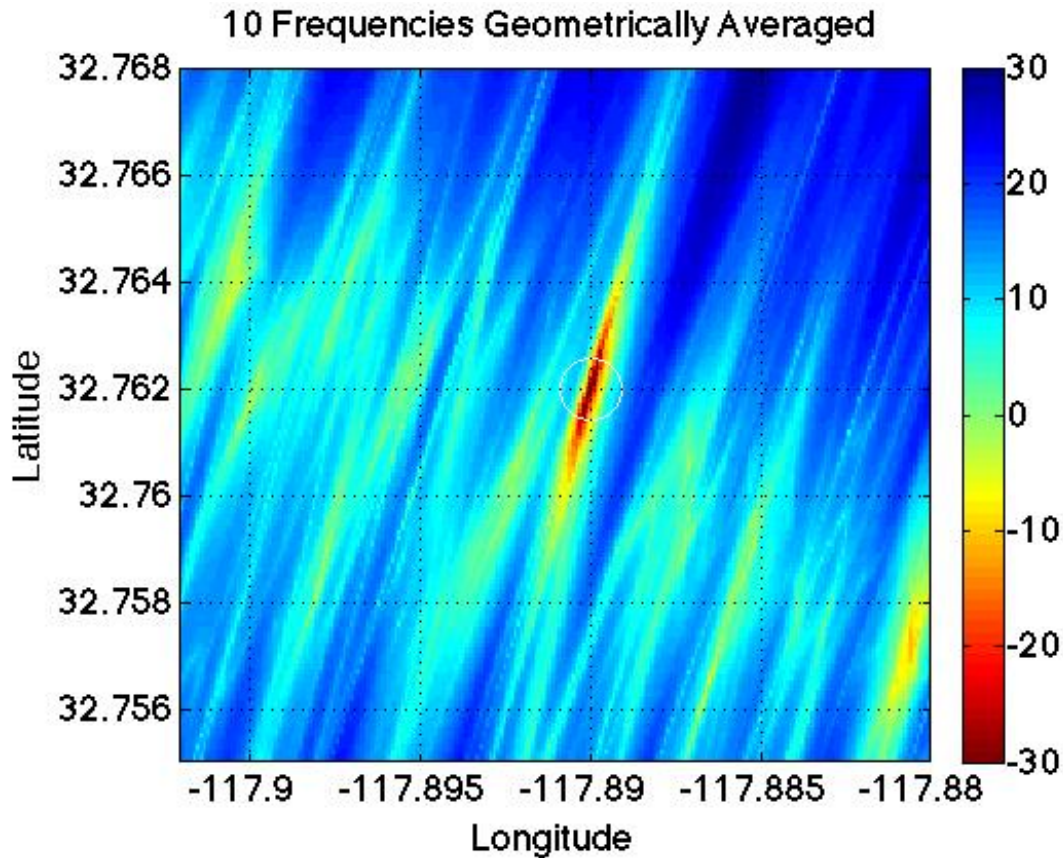
Figure 4.11: Average of Source Localization Output for 10 frequencies (Geometric Mean).

because sensors on vertical arrays are not entirely static, and it is unlikely when this method is extended to real world applications, that sources of opportunity will be available to populate every possible grid point to build a library of replicas. Due to the principal of reciprocity in acoustic signal propagation, perturbing the sensor by a small distance is analogous to moving the source position by that same amount. I experimented with moving the source position for the simulated 'data' signal off of the grid point used to create the library correlation value. The resulting localization outputs are shown in Figure 4.14.

In all cases the source localizer locate the source in a grid box adjacent to location of the source used to create the simulated 'data' signal. The final experiment to be done using the model was to determine if the method could be used for sources of differing spectral characteristics. In other words, could a
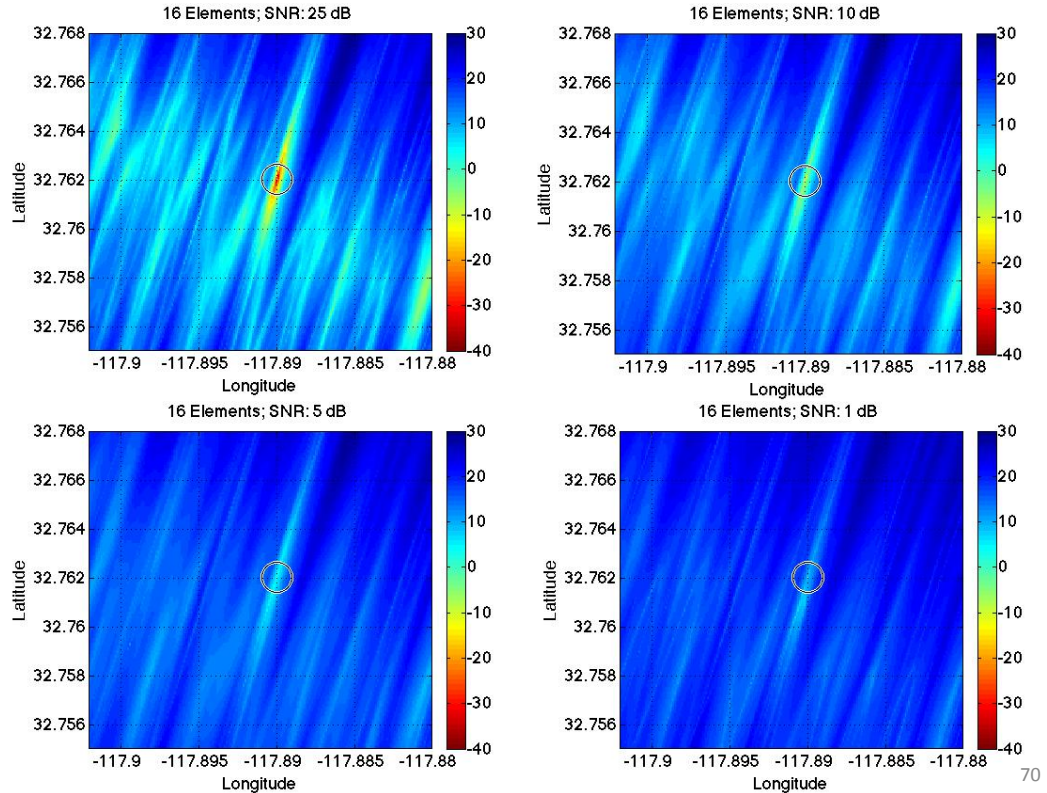
Figure 4.12: Results of source localization with 16 elements summed in the presence of noise with SNR of 25, 10, 5, and 1 dB. As anticipated, the method performs best in low noise environments, and the spatial ambiguity increases while the dynamic range of the output decreases as noise is added to the system.

library ship with one spectrum be used to find an event ship having an entirely different spectrum? Given that all ships sound different, this must work in order for this method to be applied to real source localization problems. In order to test this, I generated two time series having entirely different spectra, propagated them through the normal mode model, computed the cross-correlation, and compared the cross-correlations. Figure 4.15 shows the source localization results obtained when the library and event ship have different frequency content.

It is clear that a library of correlation vectors created using a source with certain spectral characteristics can be used to localize a source with entirely different spectral characteristics. Using simulated acoustic fields generated using a
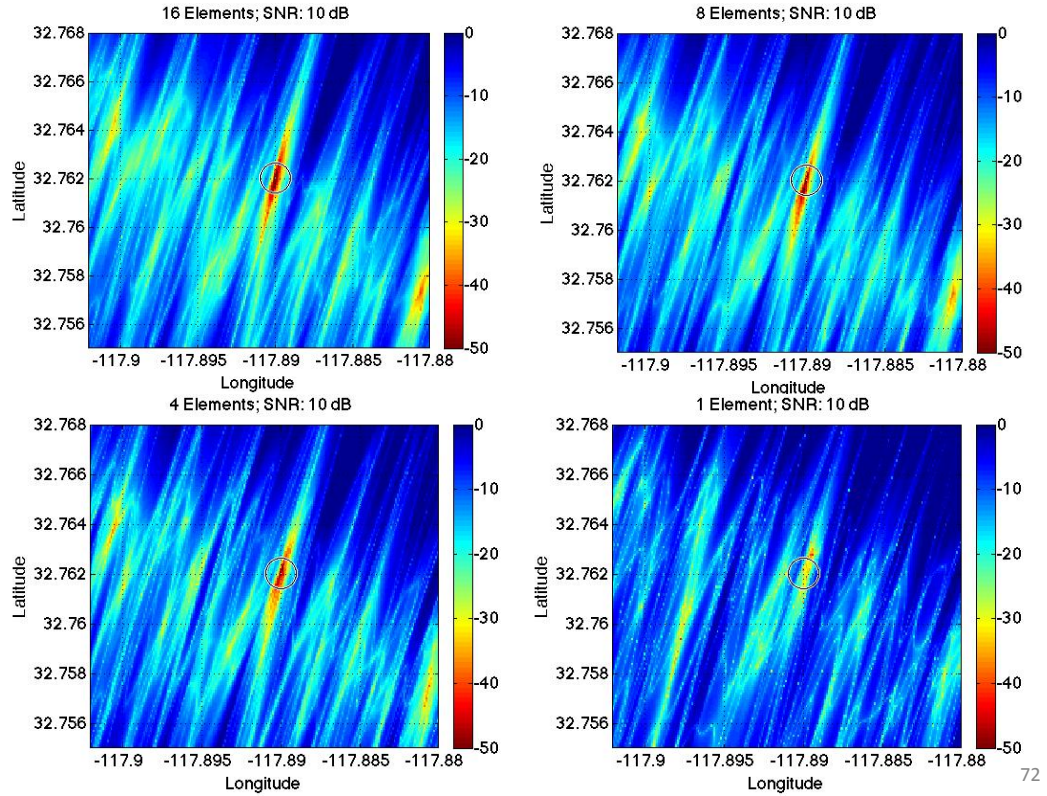
Figure 4.13: Results of source localization technique in a 10 dB SNR environment with 1, 4, 8, and 16 elements summed. As expected, the array gain increases with more elements, and the apparent SNR improves.

standard normal mode propagation model it has been shown that replica acoustic fields generated by acoustic radiators in different positions can generate correlation values unique enough to identify the position of a future unknown acoustic radiator. This suggests that the method of using measured correlation replica fields to localize acoustic sources in the ocean environment may be effective, but testing needs to be done with real data in the ocean environment to test the robustness of this system in the marine environment.

Chapter 4, in part is currently being prepared for submission for publication of the material. Verlinden, C.M.A.; Kuperman, W.A. The thesis author was the primary investigator and author of this material. Dr. William Kuperman, the
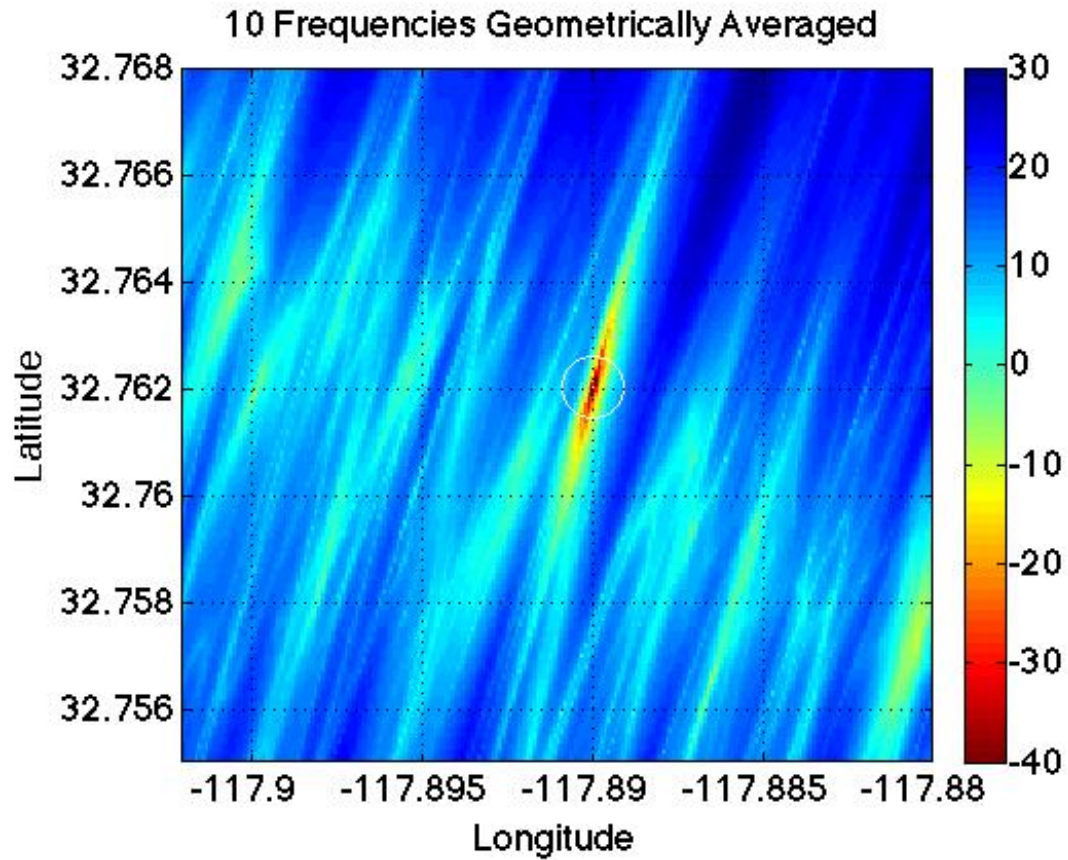
Figure 4.14: Source Localization results when the source location does not match a library grid point. The source is still effectively localized suggesting the spatial resolution used to generate the models in this problem is appropriate for the spatial scales of variability of the correlation vector.

chair of the committee, is the co-author.
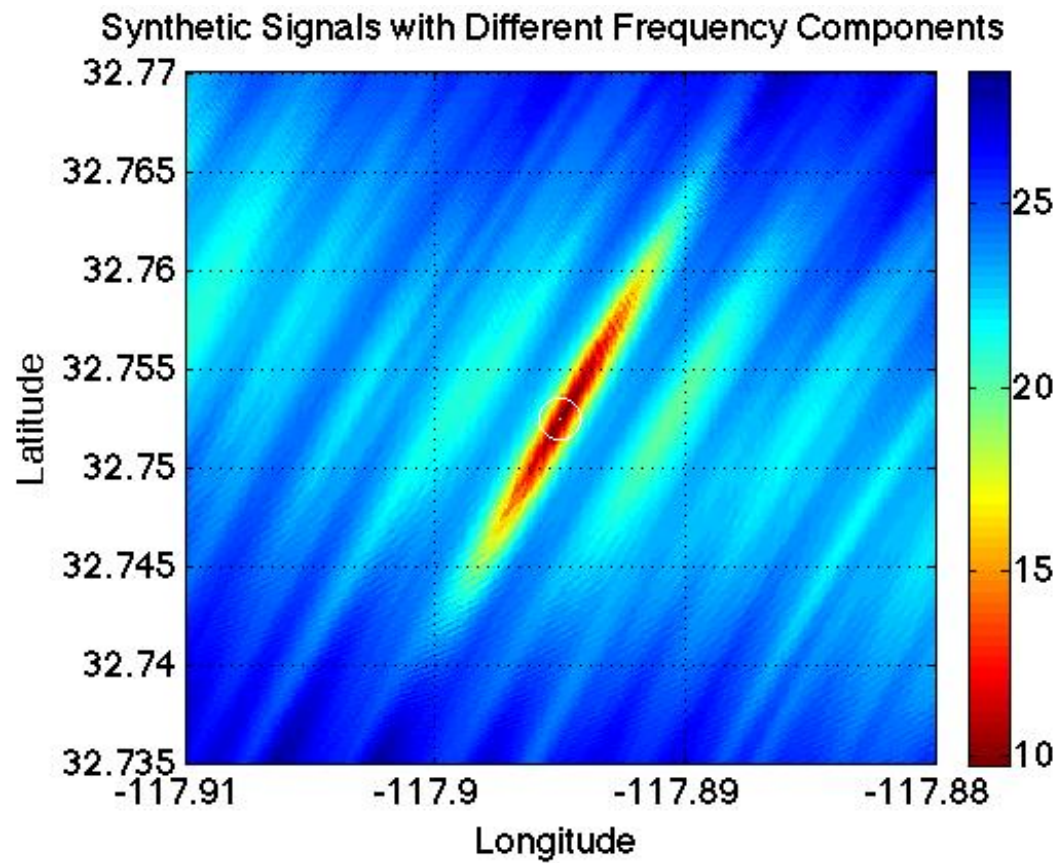
Figure 4.15: Source localization output for system using different frequencies to create library and event correlation vectors. The source is still localized in every case as long as the sampling in frequency space is not too sparse, and the spectra are computed over approximately the same band.

Chapter 5

Data

5.1 Source Localization

Once the theory has been demonstrated using simulations, it must be validated with experimental data gathered in the ocean environment. It remains to be seen whether this technique is robust enough to perform in the field with real data. As discussed in the previous chapter the experimental data that is used to validate this theory is data gathered during the Noise 09 acoustic experiment. In this experiment there were four vertical arrays with 16 elements each, approximately 15km off the coast of San Diego, CA spaced 500 m, 1000 m, and 1500 m apart. The experiment lasted 10 days, from 29 January through 06 February, and there is acoustic data for all four arrays, and ship tracking data for the entire region within 500 km of the study area for the duration of the experiment. The first step was to select a single ship track to use to populate a library of correlations, then identify a time in which a different ship crossed the library ship track, and attempt to locate the crossing using a comparison of cross-correlation vectors. In other words, for the time being I will not populate an entire grid with replica correlation vectors; rather, I will populate a single vessel track with replica correlation vectors, and attempt to localize where an when another ship crosses that track. The event I chose to focus on is illustrated in Figure 5.1. The red track is the vessel I chose to use to create the library. It is a supertanker that transited from south to north across the grid. The green track is the vessel I will be attempting to localize. It
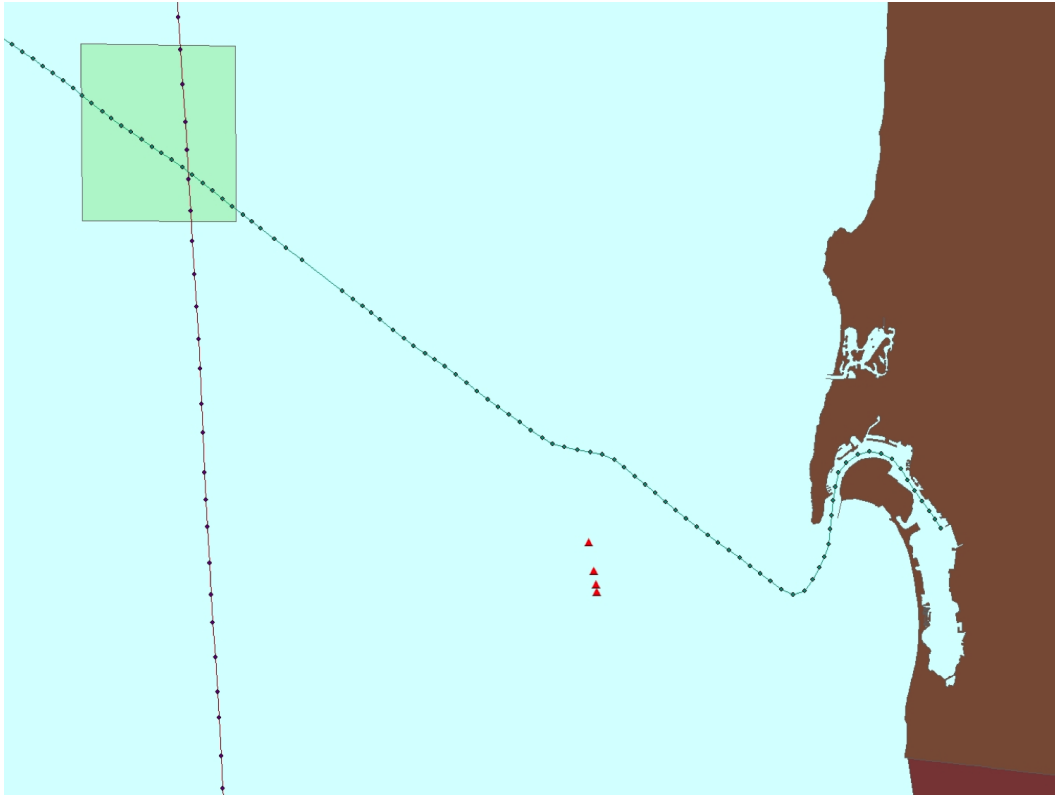
Figure 5.1: Ship tracks for library and event ship. The library ship is shown in red, and the event ship is green. The array positions are shown as red triangles. The green box represents the grid that ultimately will be populated with ship tracks.

represents a tug boat that crossed the path of the supertanker approximately 2 hours later in the day. The crossing took place approximately 40 km from the array.

In order to build the library of measured replica correlation vectors, it is easy to see that it is advantageous to ensure the signal you are cross correlating on two array elements, and associating with a grid point at the location of an acoustic radiator, are actually being generated by that radiator. There are a variety of methods to do this that will be discussed in the next section, but for the first, most simple demonstration of the concept, I will qualitatively select a library ship track for a source that is clearly dominating in correlation space. Figure 5.2 shows a plot of the cross-correlation vector in the time domain with lag time on the x-axis and time in the experiment on the y-axis. The theoretical value for the direct

arrival for a ship in the relative position, following the course and speed of library ship number 67 is superimposed. This will ensure that my library correlation vectors are being associated with the correct grid points. I do this by plotting the theoretical cross-correlation maximum peak for a direct arrival coming from all ships in the region surrounding the array, on top of the plot of the actual cross-correlation of the acoustic signal on the two array elements, over time, and look for agreement between the theoretical values of the various ships in the region and the observed cross-correlation. Figure 5.2 shows the theoretical value of the lag time for a direct arrival for ship number 67 (a super tanker) for a one hour section of the experiment superimposed over the top of the plot of the actual cross-correlation of the observed acoustic signal on the two elements over the same time period. You can see there is good agreement between the theoretical cross-correlation for ship number 67 and the observed value, so I chose to use this one hour section of data to build my library, associating the position of ship number 67 over time, with the cross-correlation vectors in the library.

The cross-correlations displayed in Figure 5.2 were calculated over intervals of 15 seconds because given the speed of the vessel in question (as determined by AIS), and the grid size calculated in the previous chapter based on the lobe thickness of the beam directivity plot for the Noise 09 array, a ship would remain in the same grid box for at least 15 seconds. Once a library and event had been chosen, the next step was to build the library of correlation vectors and assign those correlation vectors to the latitude and longitude of the library ship at the time that the correlation was computed. For the first trial I used only one element on each of the two vertical arrays (VLA1 and VLA2). I computed the library cross-correlation vectors using the same method as described in equations 3.18, 3.19, and 3.20. Note that unlike my model results which were computed for individual frequencies, in the frequency domain, this represents a broadband approach, so the cross-correlations saved for each grid point are vectors, not scalar values like they were in the simulation. After the cross-correlation values were computed for the library ship, I repeated the above same procedure for the event ship. I computed the correlation vectors for 15 second sections of data for the time when the event
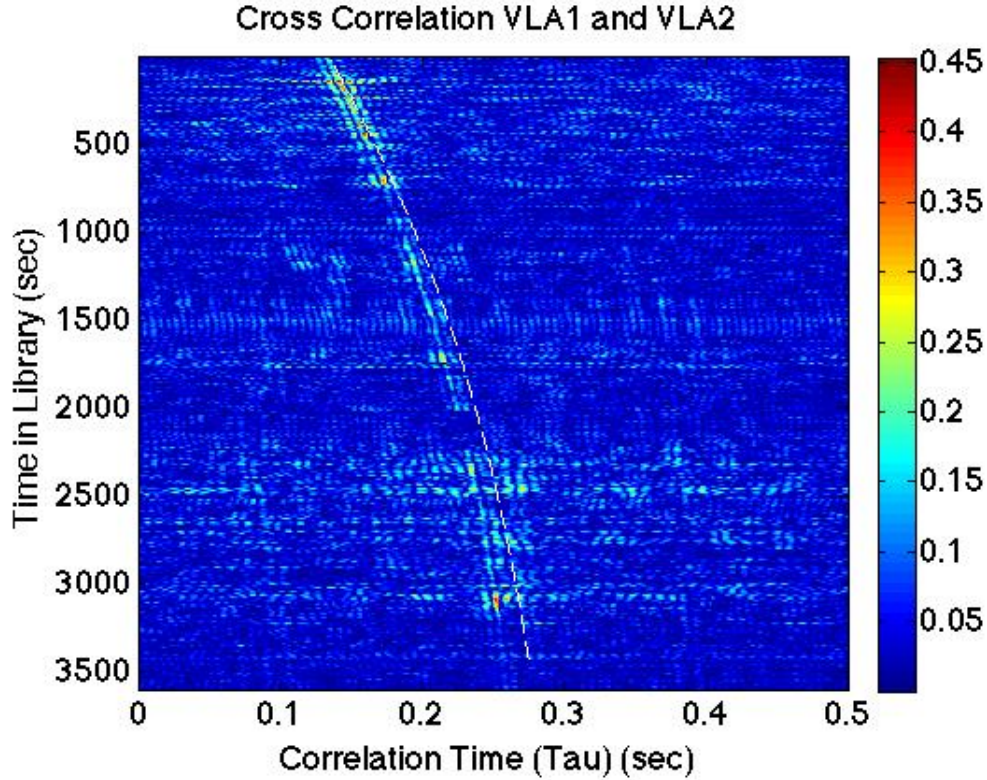
Figure 5.2: Correlation Surface for one hour library; Ship number 67 theoretical value superimposed as a dashed white line.

ship crossed the track of the library ship as well as for a few minutes on either side of the crossing event, so that I could ensure, if there was a close match during the crossing, it was not just an anomaly and correlation vectors in the library and event database would not match as closely during times when the event ship was not crossing the path of the library ship. Once the cross-correlations across the two array elements were computed for the library as well as for the event, all that remained was to compare the two. Just as with the simulation, this was done using a second cross-correlation as well as using least squares. The results that will be displayed in this section were computed using the least squares comparison method.

$$\sum (|C_{12e}(t)| - |C_{12l}(t)|)^2 \rightarrow D_{el} \qquad (5.1)$$

First I compared the correlation vectors in the library with one of the vectors

chosen from the library itself. In other words, I localized the library ship using the correlation vectors taken along its own track. I did this to test the mechanics of the program, as well as to gain insight into the spatial scales of variability and potential impacts of side lobes on the problem. Figure 5.3 shows the source localization results when the event acoustic signal is chosen from one of the library values. I compared the cross-correlations in the library with a value from the library. This will obviously show a distinct peak in the location of the library value chosen as the event value, but it also illustrates where I can expect to see side lobes and ambiguities in the results when a different ship is chosen as the event acoustic source.

Now that I have used the library to locate a value contained within in order to check my methodology, the next step is to use the library to localize a different event ship. Figure 5.4 shows the source localization output for a different ship, that crossed the track of the library vessel at precisely the time plotted in the Figure. The green 'x' shows the location where the crossing took place and there is a clear peak in that location. There is also a side lobe of equal amplitude further along the track. This side lobe appears right where the side lobe did on the plot of the library vector correlated with itself. This side lobe will be discussed further in the next chapter.

It is apparent from Figure 5.4 that there is a distinct peak in the source localization processor output where the crossing took place, at the time when the crossing took place. There is no peak in the localization output before or after the crossing. This means that with a single ship track in the library I am able to correctly localize an unknown acoustic radiator when it crosses the library ship track at a later time. This suggests that the method can be used in the ocean environment to localize sources, and that it should be possible to populate an entire grid with library measured replica correlation vectors from historical ship tracks and localize a source anywhere in that grid. Figures 5.3 and 5.4 were created using just one hydrophone on each of two vertical arrays.
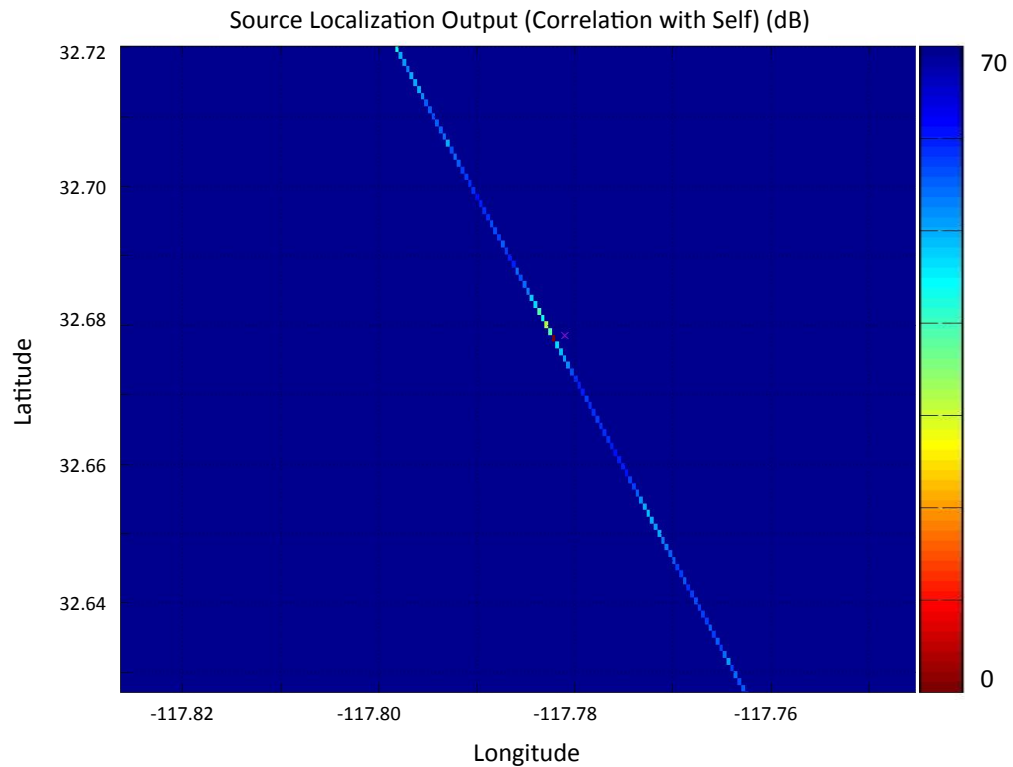
Figure 5.3: Localization of the Library ship using the replica vectors computed along its own track. As expected, there is a distinct peak in the location of the ship (next to the pink 'x'), with a region of slightly higher energy surrounding it. This indicates I chose an appropriate grid size for the spatial scale of variability of the problem. There are also side lobes with non-trivial amplitude spaced throughout the ship track.

5.2 Source Differencing Methods

You can see in the localization results in the previous section that there is some side lobe reduction from summing multiple elements, but there are still significant side lobes, some with magnitudes comparable to the primary peak. This suggests that these side lobes are not artifacts of random noise in the system, which would have been significantly reduced by the summing of multiple array elements, but rather are indicative over other nuisance signals coming from coherent sources present in the library and event acoustic data. In other words, there were other
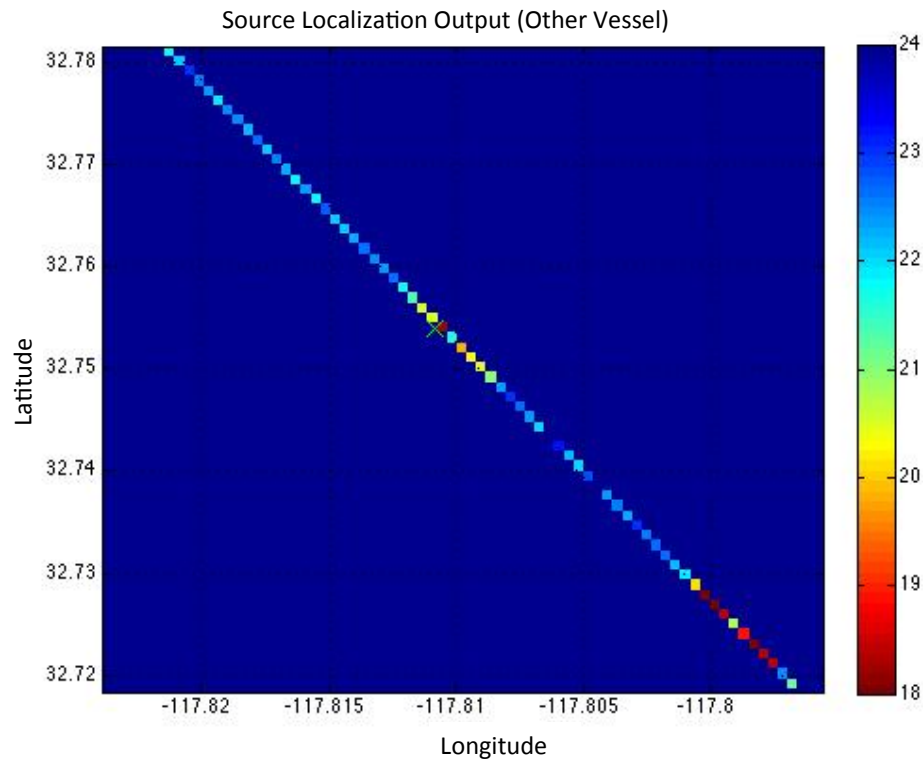
Figure 5.4: Source localization output for when a different ship crossed the track of the library track. The green 'x' represents the true location of the crossing and there is a clearly visible peak at that location during the crossing, and there is not before or after the crossing.

ships in the area when the library acoustic signals were recorded, as well as during the event data set, and the other peaks we are seeing in the correlation comparisons are likely from these nuisance signals. This concept is illustrated in Figure 5.5.

In order to eliminate these nuisance parameters from the results of the source localizer it is necessary to eliminate all superfluous signal parameters from the acoustic time series used to create the cross-correlation vectors in the library. I experimented with two methods for doing this. The first method involved selecting only the frequency bands associated with the target ship I am attempting to use for the creation of the library using a variety of methods, and the second method involved using only the portion of the cross-correlation vector associated with a
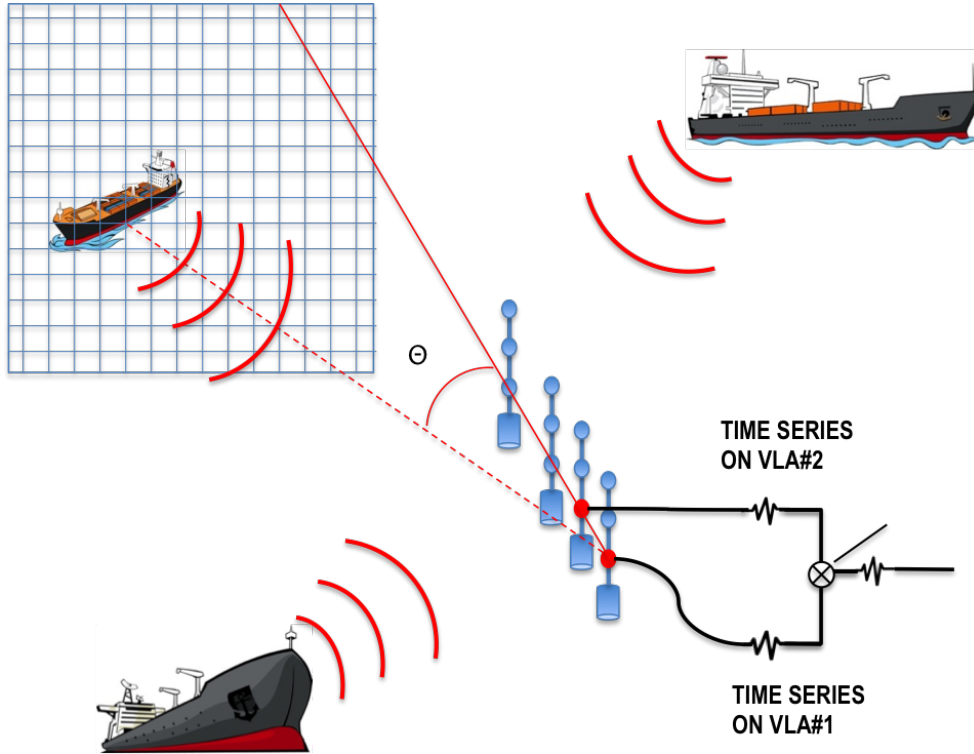
Figure 5.5: Schematic of other ships in the area interfering with the calculation of a library correlation value containing only the signal from the target library ship in the grid.

source in the general direction of the library ship for comparison in the least squares analysis. In order to reduce the influence of nuisance acoustic radiators on the result of the source localizer, it is beneficial to use only the portions of the spectrum dominated by the acoustic source you are using for your library positions in the calculation of the library cross-correlation vectors as shown in equation 5.2.

$$X_1(\omega_n)X_2(\omega_n)) \rightarrow C_{12n} \tag{5.2}$$

Identifying which frequency bands are associated with which ship can be done in a number of ways. Using AIS ship tracking data gives us access to the position of all ships in the study area, as well as information concerning the course, speed, destination, type, and dimensions of each ship. Using the course and speed information it is possible to predict the Doppler shift that each potential library ship should be experiencing at any given time due to its course and speed through

the water relative to the array elements. It is possible then to examine the spectrogram of the acoustic signals received on the array elements, and identify which tonals in the spectrum are shifting over time as one would expect for a ship with the position, course, and speed of the potential library ship. In other words, by examining the slope of individual tones on the spectrogram one can identify which tonals belong to which ship. Then in the calculation of the library cross-correlation vector is done only using the frequency bands associated with the tonals of the target library ship. While this method could be automated fairly simply, the implementation of an automated system is outside the scope of this study, which focuses primarily on proving the method as a concept. Instead of using the above, Doppler shift, method of isolating individual frequency bands associated with target library ships, I chose to use a more qualitative method for the purposes of this study. The Noise 09 experiment involved the deployment of 4 vertical arrays, each with 16 elements. In order to improve SNR, 16 elements an each array were summed together, and in order to amplify the frequency components associated with an individual target library ship the time signals on each array were added together with a time delay associated with a signal coming from the direction of the library ship. Equation 5.3 shows how to compute the theoretical time delay for the target ship between elements; equation 5.4 shows how the time series can be summed together; and equation 5.5 is simply computing the FFT of the resulting summed time series to see which frequency components are most amplified by the summation.

$$\tau_n = \frac{h_n \cos(\arctan \frac{V}{H})}{c} \tag{5.3}$$

$$S(t) = s_1(t) + s_2(t + \tau_2) + s_3(t + \tau_3) + s_4(t + \tau_4) \tag{5.4}$$

$$S(\omega) = fft(S(t)) \tag{5.5}$$

Once the time signals were summed with the time delay associated with the incoming signal from the target ship, a spectrogram was generated for the time when the library ship was in that location. The tonals on the spectrogram that
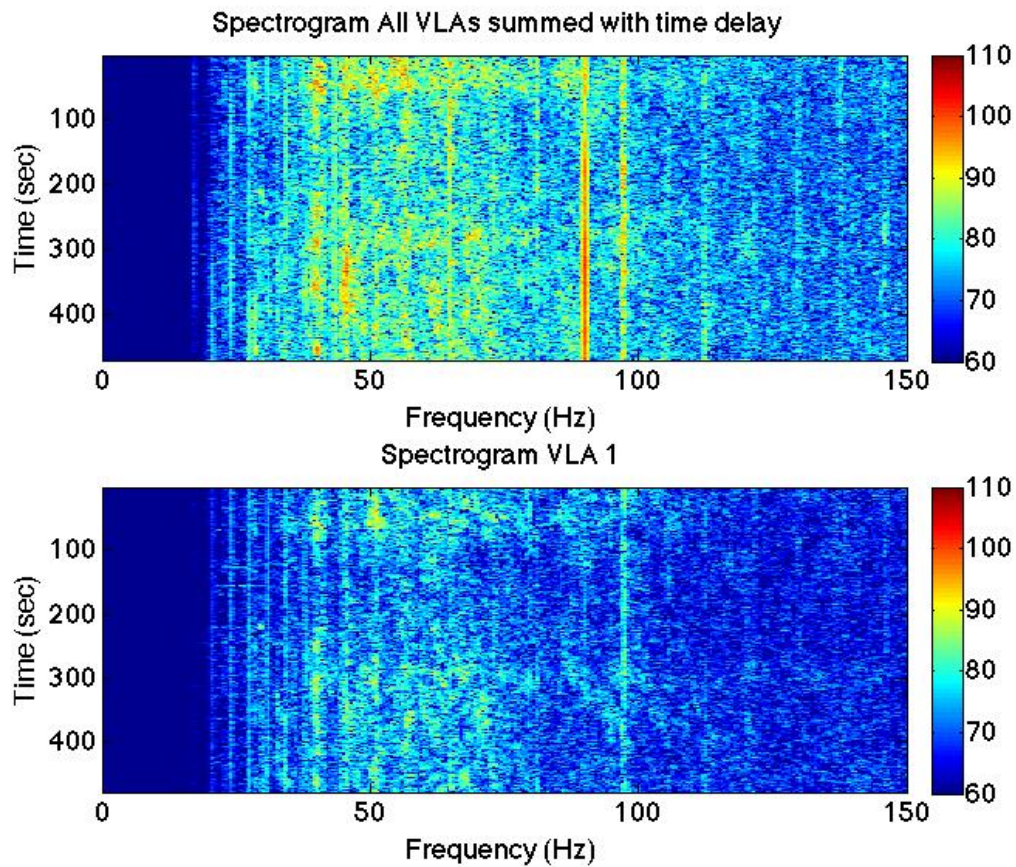
Figure 5.6: Spectrogram of all elements on VLA 1 summed (bottom). You can see several distinct tones associated with ships but it is not possible to tell which tones are associated with which ships. The top Figure shows the spectrogram after all elements on all four arrays are summed together with the time delay associated with a source in the location of the library source. It is clear that some tones, such as the 90 Hz band are amplified more than others and are therefore likely associated with the library ship.

were amplified by the summing of the four arrays with a time delay (essentially beam steering the array), were likely the tones associated with the target library ship. Figure 5.6 shows the spectrograms before and after summing with time delay.

You can see several tonals on the spectrogram were amplified when the four arrays were summed with a time delay. This procedure is analogous to beamforming in the direction of the target library ship. The tonals that were amplified are likely associated with the target library ship. Now I will select only the frequency

bands that are associated with the target library ship and use those for calculating the library cross-correlation values.

$$X_1(\omega_n)X_2(\omega_n)) \to C_{12n} \qquad (5.6)$$

I will then use these cross-correlation vectors for comparison to the data cross-correlation vectors and see how the results compare to the broadband results that used the entire frequency spectrum. For the first trial, I selected the 12 frequency bands above that were amplified the most by summing in the time domain. To ensure I captured the entire frequency band, I used 3 Hz bands centered on the center frequency of the target tonal on the spectrograms. The results of the source localizer when the library cross-correlation vectors are computed using only the 12 qualitatively selected frequency bands are included in Figure 5.7.

You can see from theFigure 5.7 that the side lobes seen in the previous results are reduced by the inclusion of only frequency bands that are likely associated with the target library ship. The method of qualitatively selecting frequency bands for the creation of the library of correlation vectors begins to break down when too few frequency bands are used and more analysis is required to determine how densely the spectrum must be sampled in order for the method to function. It is important to note that this will likely be different for every case depending on the individual spectral characteristics of different target library ships, depending on how much of the variance of the signal of the ship is contained within the frequency bands selected for localization.

The second method that is explored in this thesis for reducing the side lobes associated with nuisance acoustic sources during the experiment was the inclusion of only the portion of the library correlation vector likely associated with the target library ship by simply only using the portion of the cross-correlation vector with a lag time surrounding the theoretical lag time for a direct arrival for a source in the position of the target library ship. Essentially, the theoretical lag time for a ship in the position of the library ship was calculated as in the previous section, and then length of the impulse response of the channel (duration of the arrival structure) was added and subtracted from the theoretical lag time to determine
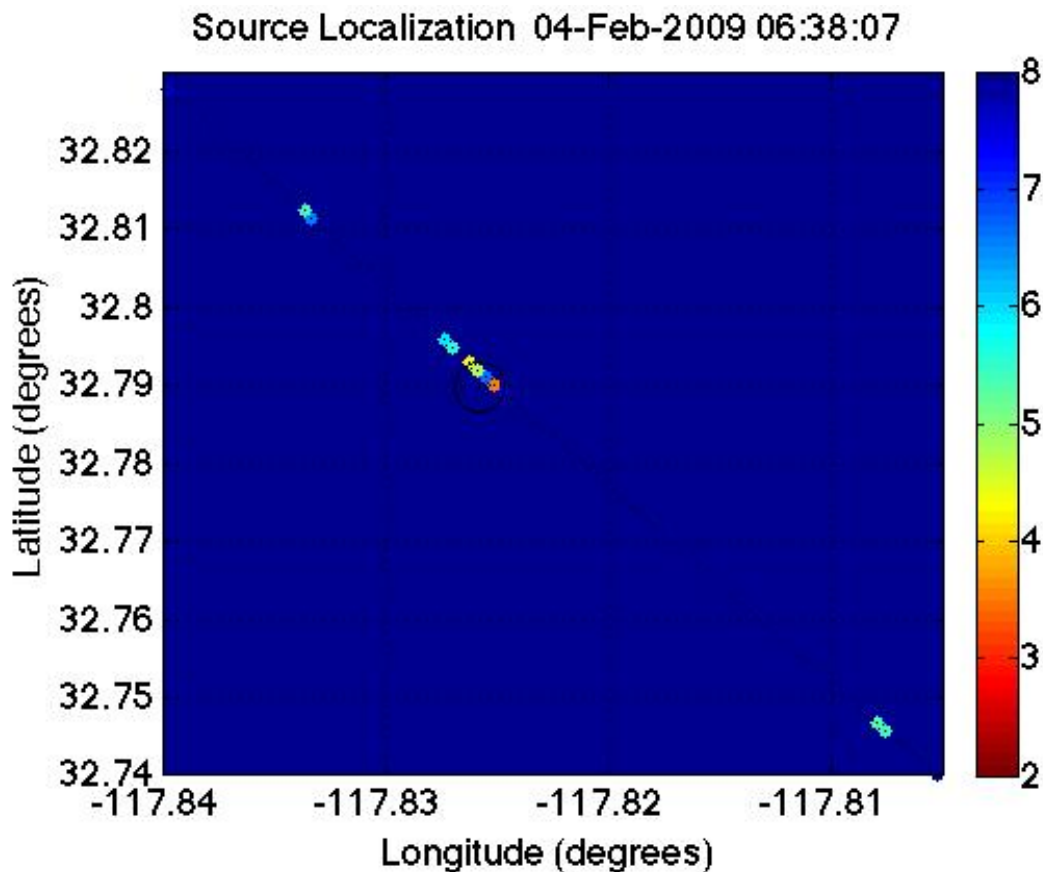
Figure 5.7: Source Localization Output (dB) for 12 frequency bands qualitatively selected as beeing associated with the library ship.

what window of the correlation function to use in localization. Figure 5.8 is a plot of the library cross-correlations with the section of each cross-correlation used for comparison to the event cross-correlation vectors highlighted in red. The same portion of the event correlation vectors are used for comparison. Results of this method of reducing the influence of nuisance acoustic sources on the localization results have been inconclusive as results appear neither improved nor deteriorated.

The correlation based source localization method using measured replica fields expounded upon in chapter 3 and demonstrated using a model in chapter 4 has been applied to acoustic data sets collected in the ocean environment, and used to identify when and where a vessel crossed the path of another vessel. These results are promising in that they suggest it is possible to populate an entire grid with correlation vectors taken from measured replicas, and continuously localize
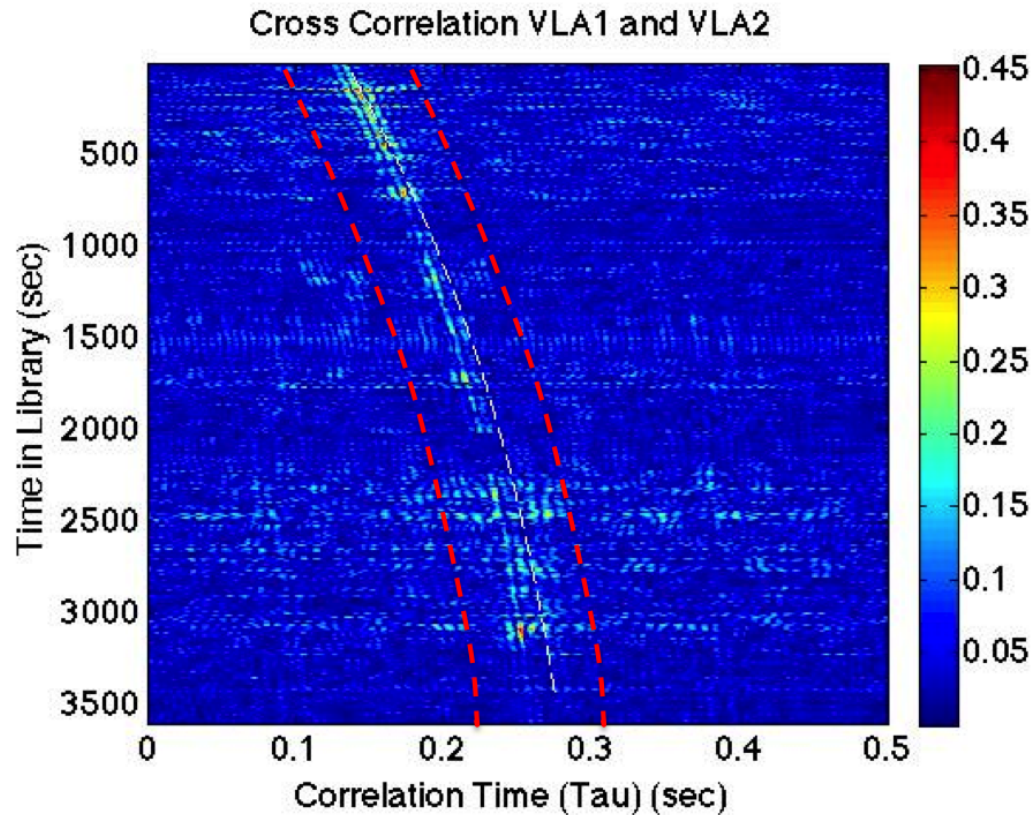
Figure 5.8: The cross-correlation of the library ship over time is plotted as a colored surface with amplitude of the correlation represented by the color bar, correlation time on the x-axis, and time in the experiment on the y-axis. The portion of the cross-correlation vector used for comparison in highlighted in red.

sources in the ocean environment.

Chapter 5, in part is currently being prepared for submission for publication of the material. Verlinden, C.M.A.; Kuperman, W.A. The thesis author was the primary investigator and author of this material. Dr. William Kuperman, the chair of the committee, is the co-author.

Chapter 6

Future Work

In order for this method to be a useful technique for localizing acoustic sources in the ocean environment there are several additional steps that need to be taken. The method must be demonstrated for more shipping events and it must be able to localize sources under a variety of circumstances with varying geometries. It needs to work when the sources are at any angle with respect to the azimuth of the array, and for sources at any range. Currently vessels that are too close to the arrays are problematic to localize because they change their relative bearing to the array so rapidly that only very short correlation times can be used for creating the correlation vectors for comparison. These short correlation times are turning out to be more difficult to use for localization and more work needs to be done in order to overcome this.

The ultimate goal is to populate an entire grid with library correlation vectors, including areas where I may have no historical ship tracks with which to correlate. This will allow an operator to continuously track contacts. In these cases I will need to interpolate correlation vectors I do have from adjacent grid points to estimate a correlation vector for those grid points as illustrated in Figure 6.1.

Unfortunately there is not a standard method for interpolating vector data in this fashion, so I will need to parameterize the data correlation vectors that I do have in terms of empirical orthogonal functions, singular value or eigenvector decompositions, or even potentially with wavelets, then interpolate the parameters
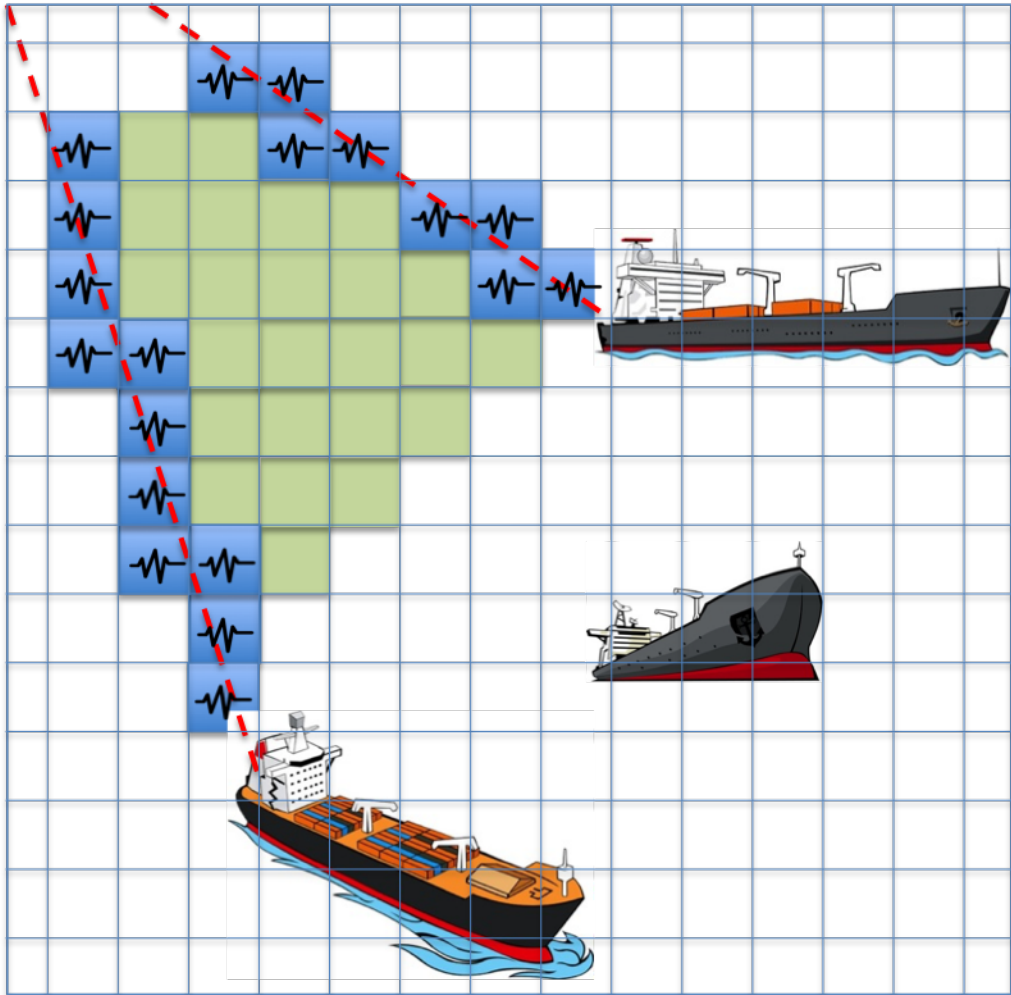
Figure 6.1: For areas where no library correlation vectors exist, correlation vectors must be constructed by developing an interpolation scheme between populated grid points in the library. In this diagram the blue squares represent grid points with associated library correlation vectors, and the green squares are the points in between that need to be filled in with some sort of interpolation scheme. One possible embodiment of an interpolation scheme is parameterizing the correlation vectors using EOFs and interpolating the eigenvalues associated with each eigenvector between points.

between grid points. In the case of the empirical orthogonal functions I would simply do a 2d linear or kriging interpolation of the coefficients associated with each EOF between points I have data for. This will involve doing some statistical analysis to determine the decorrelation length scales of these correlation vector parameters, which will need to be an adaptive process, as the decorrelation scale

will change as a function of the speed of the ship, and the bearing and distance from the array to the source of opportunity. Once the coefficients of the EOFs have been interpolated in between data points, cross-correlation vectors can be constructed from the EOFs for every position in the grid. It remains to be seen whether not parameterizing the cross-correlation functions in terms of EOFs will turn out to be an appropriate method filling in gaps between sampled library data points.

In addition to a spatial interpolation scheme, there will ultimately need to be a dead reckoning aspect to the final source localization algorithm. There will always be side lobes in methods such as this one, but the side lobes will not persist as consistently and coherently as real data. If there is a consistent high energy area moving across the localization grid, and side lobes constantly forming and disappearing around the main lobe, then the consistent high energy area is the location of the contact, and the other, less consistent regions must all be side lobes. There are a variety of methods for doing this quantitatively that have been developed for the SONAR and RADAR communities, and work needs to be done to determine which methods are most appropriately applied to this acoustic source localization method. Figure 6.2 illustrates this concept of preferentially weighting grid points that are along apparent tracks of known contacts.

Because the decorrelation length scale, as well as the integral time scale, for the correlation vectors of sources in different positions in the grid are different, depending on the position with respect to the array elements, the speed of the ship, and the differences in the local green's function / transfer function of the medium, the characteristics of the grid will have to be adaptive. This means the resulting resolution, accuracy, and reliability of the source localizer will change spatially, and in time as the number, location, speed, and characteristics of the library ships changes. Additionally, it is difficult to predict how old data used in the library can be before it is no longer representative of the signal one could expect for a ship in a given location. Changing ocean waveguide characteristics with seasonal, diurnal, tidal, and internal wave phenomena can all invalidate the correlation vectors used for source localization. If these phenomena change the transfer function (Green's
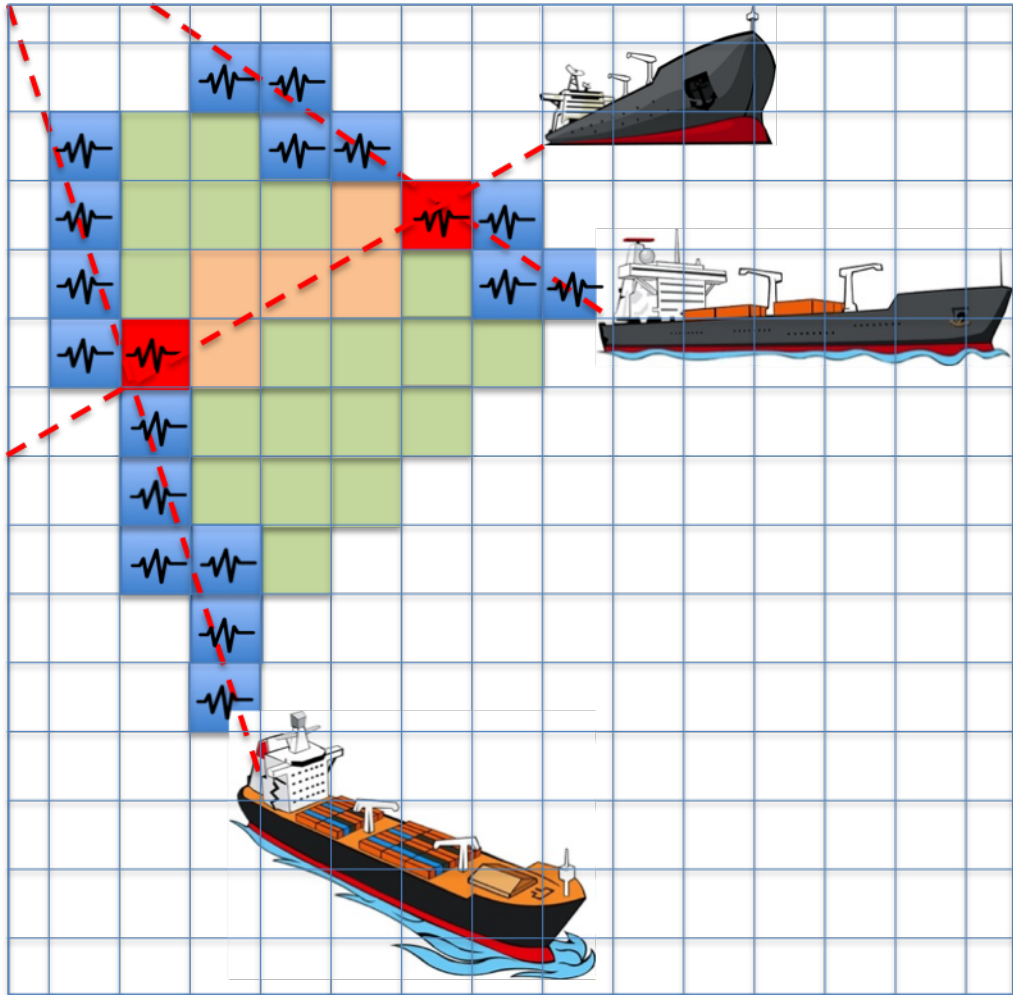
Figure 6.2: In order to properly localize the source in the presence of side lobes that will inevitably persist to some level in this method, a method of vessel tracking using dead-reckoning or 'track-before-detect' methods must be used. In other words if there is a major peak when the target vessel crosses one populated library track, then another peak moments later on a different library track, then the target must be moving in between those two tracks, and greater weight should be placed on that region.

function) of the waveguide between source and receiver sufficiently, one would no longer expect the correlation vectors of ships in that position at different times to correlate well. In the data used in this experiment, data from the same day were always used, and while this did not seem to be an issue, that may not always be the case. Data from previous days and even weeks could be used, and this subject

requires additional research. Phenomena and circumstances that impact when it is appropriate to use data from previous days should be quantitatively examined. It is also possible to use adaptive processing to check replica values for coherence with other replicas before determining whether or not to use a particular replica value in the localization of a target at a given time.

There is also more work that can be done isolating signals generated by desired ships in the creation of the library of correlation vectors. This field is sometimes called 'Blind Source Separation', but in this case that turns out to be a misnomer. In this case we have a great deal of knowledge about our acoustic radiators taken from AIS ship tracking data, that can be used to help us separate sources. It is conceivable to beamform in the direction of the library ship and correlated only the beamformer output in the creation of the library. This would require a full horizontal or volumetric array, however with appropriate element spacing for the frequency range being used for the beamforming, and in this experiment we used only two elements separated by over 500 meters, so beamforming was not possible. There are two other methods to selectively identify ships to use in the creation of the library of replica correlation vectors that are explored in this paper and require further research to be implemented in a robust manner. The first involves summing the time domain signals received on multiple elements on each of the four vertical arrays with the appropriate estimated time delay associated with the arrivals to each element for a source in the location of the library ship. The spectrum of the summed, time-delayed, signal can then be analyzed. The frequency bands where this signal is strongly coherent (i.e. tonals in the spectrogram) can then be used selectively in the calculation of the cross-correlation used in the creation of the library. This is essentially analogous to setting a preferential 'listening' direction for the creation of the library. I experimented with this method in this thesis, but more work remains to be done to determine feasibility and implementation in the field; specifically how many frequency bands are required, and quantifying what signal to noise ratio benefits might result from this method. The second method for preferentially favoring desired ships' signals in the creation of the correlation library that I experimented with is to simply cut

out the portion of the correlation vector with the expected lag time for a source in the location of the library ship and only use that portion of the correlation in the differencing scheme (least squares or cross-correlation) between the library and event correlation vectors. I have experimented with using this method with some limited success, but more work should be done to determine how feasible and appropriate this method is. Other potential methods of source separation that should be explored are Doppler based methods, that use the Doppler shift of individual sources to separate sources. Given that we have *a priori* knowledge about the course, speed, and location of all acoustic radiators in the band we are concerned with, we should be able to determine which portions of the signal comes from which source based on the expected Doppler shift. Blind source separation represents an entire field in passive acoustics and more work needs to be done to determine which existing methods should be applied to this source localization method.

Chapter 7

Conclusion

There are a number of acoustic sources of opportunity that are currently underutilized in the field of underwater acoustics. Specifically, advances in ship-tracking technology has made determining the location of acoustic radiators in the open ocean far more accessible, and this ship-tracking data can be applied in a variety of meaningful applications in ocean acoustics. In this thesis, I discussed one particular application in depth: the use of AIS vessel tracking data in passive acoustic source localization through correlation processing using measured replica fields, as well as proposed some potential future applications of ship tracking data in passive acoustics.

Using the cross-correlation of the acoustic signal across two or more elements on arrays separated by an arbitrary horizontal distance, I was able to demonstrate that other acoustic sources, such as ships of unknown position, can be localized. The technique, similar to matched field processing, compares replica correlation vectors to the correlation vector during a particular event you are trying to localize the source of. The primary difference between traditional matched field processing and this technique, aside from the use of correlation vectors in place of the acoustic signal itself for matching, is the use of measured replica fields, populated using ships as sources of opportunity. The replica vectors are taken from a library of correlation vectors calculated when ships were in certain locations, and associated with the latitude and longitude of the ships/sources. While further work remains to be done before this method can be applied in robust field appli-

cations to localize acoustic sources in any location in a desired grid, it has been demonstrated using models, and experimental data from open-ocean experiments, that it can be determined when an unknown acoustic radiator crosses the historical ship path used to build the library of correlation vectors.

This study is applicable to research that focuses on extracting the Green's function of an ocean waveguide using passive techniques. The theory behind this source localization technique relies upon the uniqueness of the transfer function between each point on the grid and the array. The signal received on the array can be thought of as the convolution of the signal generated by the ship and the transfer function (Green's function) of the waveguide between the source and receiver. In the case of this localization the signal of the individual ship can be thought of as a nuisance parameter as the spectrum of this signal is likely very different between ships, and as a result not coherent between the ship used to create the library and the ship localized. It is the transfer function of the medium that makes the signal, and by extension the cross-correlation of the signal on multiple elements, a unique 'fingerprint' for a source in a given location. If this transfer function is present in the correlation vector with enough power to localize a source, it means that it is likely possible to extract this transfer function using passive sources of opportunity such as ships. This would represent a significant advancement in the field of passive underwater acoustics, and is the subject of a great deal of current research. This source localization technique should be encouraging to scientists looking for ways to extract the Green's Function of ocean waveguides using passive techniques.

In conclusion, the Correlation Based Source Localization using Measured Replica Fields technique shows promise but requires more research before it can be implemented easily in practice.

Bibliography

[1] M. Siderius, C. H. Harrison, and M. B. Porter. A passive fathometer technique for imaging seabed layering using ambient noise. *The Journal of the Acoustical Society of America*, 120(3):1315, 2006.

[2] S. E. Fried, W. A. Kuperman, K. G. Sabra, and P. Roux. Extracting the local Green's function on a horizontal array from ambient ocean noise. *The Journal of the Acoustical Society of America*, 124(4):EL183–8, October 2008.

[3] P. Roux, W. A. Kuperman, and K. G. Sabra. Ocean acoustic noise and passive coherent array processing. *Comptes Rendus Geoscience*, 343(8-9):533–547, September 2011.

[4] A. B. Baggeroer, W. A. Kuperman, and P. N. Mikhalevsky. An overview of matched field methods in ocean acoustics. *IEEE Journal of Oceanic Engineering*, 18(4):401–424, 1993.

[5] M. J. Buckingham, B. V. Berkhout, and S. A. L. Glegg. Imaging the Ocean with Ambient Noise. *Journal of the Acoustic Society of America*, 356(March):327–329, 1992.

[6] P. Roux and W. A. Kuperman. Extracting coherent wave fronts from acoustic ambient noise in the ocean. *The Journal of the Acoustical Society of America*, 116(4):1995, 2004.

[7] A. M. Thode, G. L. D'Spain, and W. A. Kuperman. Matched-field processing, geoacoustic inversion, and source signature recovery of blue whale vocalizations. *The Journal of the Acoustical Society of America*, 107(3):1286–300, March 2000.

[8] A. Tolstoy, O. Diachok, and L. N. Frazer. Acoustic tomography via matched field processing. *The Journal of the Acoustical . . .*, pages 1119–1127, 1991.

[9] F. B. Jensen, W. A. Kuperman, M. B. Porter, and H. Schmidt. *Computational ocean acoustics*. American Institute of Physics, Woodbury, NY, 1994.

[10] L. T. Fialkowski, M. D. Collins, W. A. Kuperman, J. S. Perkins, L. J. Kelly, A. Larsson, J. A. Fawcett, and L. H. Hall. Matched-field processing using measured replica fields. *The Journal of the Acoustical Society of America*, 107(2):739–46, February 2000.

[11] H. Cox, R. M. Zeskind, and M. Myers. A subarray approach to matched field processing. *Journal of the Acoustical Society of America*, 87(May):168–178, 1990.